

## Assembly of $[(\eta^5\text{-C}_5\text{Me}_5)\text{MoS}_3\text{Cu}_3]$ -Supported One-Dimensional Chains with Single, Double, Triple, and Quadruple Strands

Wen-Hua Zhang,<sup>†,‡</sup> Ying-Lin Song,<sup>§</sup> Zhen-Hong Wei,<sup>†</sup> Ling-Ling Li,<sup>†</sup> Yu-Jian Huang,<sup>†</sup> Yong Zhang,<sup>†</sup> and Jian-Ping Lang<sup>\*,†,‡</sup>

School of Chemistry and Chemical Engineering, Suzhou University, Suzhou 215123, Jiangsu, People's Republic of China, State Key Laboratory of Organometallic Chemistry, Shanghai Institute of Organic Chemistry, Chinese Academy of Sciences, Shanghai 200032, People's Republic of China, and School of Physical Science and Technology, Suzhou University, Suzhou 215006, Jiangsu, People's Republic of China

Received February 25, 2008

The construction of a new set of  $[(\eta^5\text{-C}_5\text{Me}_5)\text{MoS}_3\text{Cu}_3]$ -based supramolecular compounds with different one-dimensional (1D) arrays from two preformed clusters  $[\text{PPh}_4][(\eta^5\text{-C}_5\text{Me}_5)\text{MoS}_3(\text{CuX})_3]$  ( $\text{X} = \text{Br}$  (**1a**),  $\text{NCS}$  (**1b**)) with 1,2-bis(4-pyridyl)ethane (bpe) and 1,3-bis(4-pyridyl)propane (bpp) is presented. Reactions of **1a** with bpe in different molar ratios afforded  $\{[(\eta^5\text{-C}_5\text{Me}_5)\text{MoS}_3\text{Cu}_3]_2(\mu\text{-bpe})_{3.5}\text{Br}_4\} \cdot \text{MeCN}_n$  (**2**),  $\{[(\eta^5\text{-C}_5\text{Me}_5)\text{MoS}_3\text{Cu}_3]_2(\mu\text{-bpe})_3\text{Br}_4\} \cdot \text{Sol}_n$  (**3a**:  $\text{Sol} = \text{DMSO} \cdot 3\text{MeCN}$ ; **3b**:  $\text{Sol} = 2\text{aniline} \cdot 3\text{MeCN}$ ),  $\{[(\eta^5\text{-C}_5\text{Me}_5)\text{MoS}_3\text{Cu}_3]_2(\mu\text{-bpe})_3(\text{bpe})\text{Br}_4\} \cdot 0.35\text{DMF}_n$  (**4**), and  $\{[(\eta^5\text{-C}_5\text{Me}_5)\text{MoS}_3\text{Cu}_3]_2(\mu\text{-bpe})_2(\mu\text{-Br})(\mu_3\text{-Br})\text{Br}_2\} \cdot \text{DMF} \cdot \text{MeCN}_n$  (**5**). On the other hand, treatment of **1a** or **1b** with bpp produced  $[(\eta^5\text{-C}_5\text{Me}_5)\text{MoS}_3\text{Cu}_3](\mu\text{-bpp})(\mu\text{-Br})\text{Br}_n$  (**6**) and  $\{[(\eta^5\text{-C}_5\text{Me}_5)\text{MoS}_3\text{Cu}_3]_2(\mu\text{-bpp})_3(\mu\text{-NCS})_2(\text{NCS})\}(\text{NCS})_n$  (**7**). Compounds **2–7** have been characterized by elemental analysis, UV–vis spectroscopy, IR spectroscopy,  $^1\text{H}$  NMR, and X-ray analysis. In **2**, each  $[(\eta^5\text{-C}_5\text{Me}_5)\text{MoS}_3\text{Cu}_3]$  core serves as an angular two-connecting node to link other equivalent cores by single and double bpe bridges to form a 1D “Great Wall”-like chain. In **3a** and **3b**, the  $[(\eta^5\text{-C}_5\text{Me}_5)\text{MoS}_3\text{Cu}_3]$  cores are linked alternatively by single and double bpe bridges to give a 1D zigzag chain. In **4**, six cluster cores (two as a two-connecting node and four as a three-connecting node) are connected by four single bpe and two double bpe bridges to form a cyclohexane-shaped repeating unit, which is further fused with other units to generate a 1D double-stranded chain. Compound **5** has a simple 1D zigzag chain consisting of the cluster cores linked by single bpe bridges. In **6**, the cluster cores are linked by single bpp bridges to give a 1D helical chain, which further holds two symmetry-related chains through  $\text{C-H} \cdots \text{Br}$  hydrogen-bonding interactions, thereby forming a 1D H-bonded triple-stranded chain. Compound **7** has a rare 1D quadruple chain, in which the  $[(\eta^5\text{-C}_5\text{Me}_5)\text{MoS}_3\text{Cu}_3]$  cores work as planar four- and five-connecting nodes to interconnect other equivalent cores through single bpp bridges and single and double thiocyanate bridges. In addition, the third-order nonlinear optical properties of **1a**, **2**, **3a**, and **4–7** in aniline were also investigated by using the Z-scan technique with a 4.5 ns pulse laser at 532 nm.

### Introduction

Metal–polymeric complexes with one-dimensional (1D) arrays have currently received much attention because of their fascinating structural forms (linear,<sup>1–3</sup> zigzag,<sup>4</sup> ladder,<sup>5</sup> braid,<sup>6</sup> tube,<sup>7</sup> helix,<sup>8–11</sup> etc.) and their potential applications in

magnetic,<sup>4a–g,5a,b</sup> electrophotonic,<sup>4h,5c–e</sup> biorelated materials,<sup>9c–e</sup> and sensor technologies.<sup>7a,b</sup> Metal–ligand coordination or other weak interactions such as hydrogen-bonding interactions and

\* To whom correspondence should be addressed. E-mail: jplang@suda.edu.cn. Fax: 86-512-65880089.

<sup>†</sup> School of Chemistry and Chemical Engineering, Suzhou University.

<sup>‡</sup> Shanghai Institute of Organic Chemistry.

<sup>§</sup> School of Physical Science and Technology, Suzhou University.

(1) (a) Zheng, N. F.; Bu, X. H.; Lu, H. W.; Chen, L.; Feng, P. Y. *J. Am. Chem. Soc.* **2005**, *127*, 14990–14991. (b) Takaishi, S.; Yamashita, M.; Matsuzaki, H.; Okamoto, H.; Tanaka, H.; Kuroda, S.; Goto, A.; Shimizu, T.; Takenobu, T.; Iwasa, Y. *Chem. Eur. J.* **2008**, *14*, 472–477. (c) Jia, C. Y.; Liu, S. X.; Ambrus, C.; Neels, A.; Labat, G.; Decurtins, S. *Inorg. Chem.* **2006**, *45*, 3152–3154. (d) Suijkerbuijk, B. M. J. M.; Tooke, D. M.; Spek, A. L.; van Koten, G.; Gebbink, R. J. M. K. *Chem. Asian. J.* **2007**, *2*, 889–903. (e) Barnett, S. A.; Champness, N. R.; Wilson, C. *Eur. J. Inorg. Chem.* **2005**, 1572–1576.

aromatic stacking effects are usually employed to prepare such polymers, which involves the judicious selection of metal ions and special bridging ligands. However, formation of metal–polymeric complexes only at the one-dimensional level is difficult because a single metal center always has many coordination sites available, which tends to be connected with bridging ligands to form two-dimensional (2D) or three-dimensional (3D) structures. To tackle this problem, one strategy is to introduce a bulky ancillary ligand at the metal center or metal cluster core to block some of their coordination sites. For example, reactions of  $\text{Cu}(\text{NO}_3)_2 \cdot 6\text{H}_2\text{O}$  in MeOH with a bulky Tp-coordinated

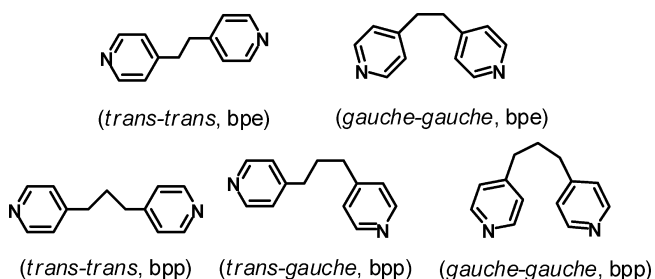
complex  $[(\text{Tp})\text{Fe}^{\text{III}}(\text{CN})_3]^-$  (Tp = hydridotris(pyrazol-1-yl)borate) afforded a heterobimetallic polymer complex with a zigzag chain structure,  $[(\text{Tp})_2\text{Fe}^{\text{III}}_2(\text{CN})_6\text{Cu}(\text{CH}_3\text{OH}) \cdot 2\text{CH}_3\text{OH}]_n$ .<sup>4b</sup> Another example is that treatment of *cis*- $[\text{Re}_6(\mu_3\text{-Se})_8(\text{PPh}_3)_4(4,4'\text{-bipy})_2](\text{SbF}_6)_2$  with equimolar or excess  $\text{Cd}(\text{NO}_3)_2$  in  $\text{CH}_2\text{Cl}_2/\text{MeOH}$  gave rise to two cluster-based polymer complexes  $[\{\text{Re}_6(\mu_3\text{-Se})_8(\text{PPh}_3)_4(4,4'\text{-bipy})_2\}_2\{\text{Cd}(\text{NO}_3)_2\}](\text{SbF}_6)_4$  (1D chain of corner-sharing squares) and  $[\{\text{Re}_6(\mu_3\text{-Se})_8(\text{PPh}_3)_4(4,4'\text{-bipy})_2\}_2\{\text{Cd}(\text{NO}_3)_2\}](\text{NO}_3)$  (1D zigzag chain).<sup>4j,k</sup>

On the other hand, the molybdenum–copper–sulfur or tungsten–copper–sulfur cluster compounds derived from  $[\text{MS}_4]^{2-}$  and  $[(\eta^5\text{-C}_5\text{Me}_5)\text{MS}_3]^-$  (M = Mo, W) have remained as an interesting topic of cluster research due to their diverse structural chemistry<sup>12–24</sup> and their relevance to biological systems<sup>21,22</sup> and photonic materials.<sup>15,16e–g,17,18e,19,20b,g–i,23,24</sup> Because some M/Cu/S clusters contain terminal halides or pseudohalides or solvent molecules coordinated at copper(I) centers that can be readily replaced by strong donor ligands

- (2) (a) Yoo, J.; Wernsdorfer, W.; Yang, E.; Nakano, M.; Rheingold, A. L.; Hendrickson, D. N. *Inorg. Chem.* **2005**, *44*, 3377–3379. (b) Prins, F.; Pasca, E.; de Jongh, L. J.; Kooijman, H.; Spek, A. L.; Tanase, S. *Angew. Chem., Int. Ed.* **2007**, *46*, 6081–6084. (c) Jin, Y.; Che, Y. X.; Batten, S. R.; Chen, P. K.; Zheng, J. M. *Eur. J. Inorg. Chem.* **2007**, 1925–1929. (d) Yamashita, M.; Kawakami, D.; Matsunaga, S.; Nakayama, Y.; Sasaki, M.; Takaiishi, S.; Iwahori, F.; Miyasaka, H.; Sugiura, K.; Wada, Y.; Miyamae, H.; Matsuzaki, H.; Okamoto, H.; Tanaka, H.; Marumoto, K.; Kuroda, S. *Angew. Chem., Int. Ed.* **2004**, *43*, 4763–4767. (e) Sun, Y. H.; Ye, K. Q.; Zhang, H. Y.; Zhang, J. H.; Zhao, L.; Li, B.; Yang, G. D.; Yang, B.; Wang, Y.; Lai, S. W.; Che, C. M. *Angew. Chem., Int. Ed.* **2006**, *45*, 5610–5613. (f) Yi, J.; Miyabayashi, T.; Ohashi, M.; Yamagata, T.; Mashima, K. *Inorg. Chem.* **2004**, *43*, 6596–6599.
- (3) (a) Wang, X. L.; Qin, C.; Wang, E. B.; Xu, L. *Cryst. Growth Des.* **2006**, *6*, 2061–2065. (b) Sagué, J. L.; Fromm, K. M. *Cryst. Growth Des.* **2006**, *6*, 1566–1568. (c) Yi, X. Y.; Liu, B.; Jimenez-Aparicio, R.; Urbanos, F. A.; Gao, S.; Xu, W.; Chen, J. S.; Song, Y.; Zheng, L. M. *Inorg. Chem.* **2005**, *44*, 4309–4314. (d) Martin, J. D.; Hess, R. F.; Boyle, P. D. *Inorg. Chem.* **2004**, *43*, 3242–3247. (e) Bosch, E.; Barnes, C. L. *Inorg. Chem.* **2002**, *41*, 2543–2547. (f) Zheng, L. M.; Gao, S.; Yin, P.; Xin, X. Q. *Inorg. Chem.* **2004**, *43*, 2151–2156. (g) Zhou, H.; Strates, K. C.; Muñoz, M. Á.; Little, K. J.; Pajeroski, D. M.; Meisel, M. W.; Talham, D. R.; Lachgar, A. *Chem. Mater.* **2007**, *19*, 2238–2246. (h) Garcia-Couceiro, U.; Olea, D.; Castillo, O.; Luque, A.; Roman, P.; de Pablo, P. J.; Gomez-Herrero, J.; Zamora, F. *Inorg. Chem.* **2005**, *44*, 8343–8348.
- (4) (a) Yin, P.; Gao, S.; Zheng, L. M.; Xin, X. Q. *Chem. Mater.* **2003**, *15*, 3233–3236. (b) Wang, S.; Zuo, J. L.; Gao, S.; Song, Y.; Zhou, H. C.; Zhang, Y. Z.; You, X. Z. *J. Am. Chem. Soc.* **2004**, *126*, 8900–8901. (c) Yuan, M.; Gao, S.; Sun, H. L.; Su, G. *Inorg. Chem.* **2004**, *43*, 8221–8223. (d) Liu, F. T.; Fu, D.; Gao, S.; Zhang, Y. Z.; Sun, H. L.; Su, G.; Liu, Y. J. *J. Am. Chem. Soc.* **2003**, *125*, 13976–13977. (e) Yoon, J. H.; Kim, H. C.; Hong, C. S. *Inorg. Chem.* **2005**, *44*, 7714–7716. (f) Kim, J. H.; Yoo, H. S.; Koh, E. K.; Kim, H. C.; Hong, C. S. *Inorg. Chem.* **2007**, *46*, 8481–8483. (g) Yoon, J. H.; Lim, J. H.; Choi, S. W.; Kim, H. C.; Hong, C. S. *Inorg. Chem.* **2007**, *46*, 1529–1531. (h) Zhao, Z. J.; Xu, X. J.; Wang, H. B.; Lu, P.; Yu, G.; Liu, Y. Q. *J. Org. Chem.* **2008**, *73*, 594–602. (i) Peedikakkal, A. M. P.; Vittal, J. J. *Cryst. Growth Des.* **2008**, *8*, 375–377. (j) Selby, H. D.; Orto, P.; Carucci, M. D.; Zheng, Z. P. *Inorg. Chem.* **2002**, *41*, 6175–6177. (k) Selby, H. D.; Roland, B. K.; Zheng, Z. P. *Acc. Chem. Res.* **2003**, *36*, 933–944.
- (5) (a) Li, L. C.; Liao, D. Z.; Jiang, Z. H.; Yan, S. P. *Inorg. Chem.* **2002**, *41*, 1019–1021. (b) You, Y. S.; Kim, D.; Do, Y.; Oh, S. J.; Hong, C. S. *Inorg. Chem.* **2004**, *43*, 6899–6901. (c) Screen, T. E. O.; Thorne, J. R. G.; Denning, R. G.; Bucknall, D. G.; Anderson, H. L. *J. Am. Chem. Soc.* **2002**, *124*, 9712–9713. (d) Agou, T.; Kobayashi, J.; Kawashima, T. *Org. Lett.* **2006**, *8*, 2241–2244. (e) Zhang, G. Q.; Yang, G. Q.; Ma, J. S. *Cryst. Growth Des.* **2006**, *6*, 1897–1902. (f) Hartley, C. S.; Elliott, E. L.; Moore, J. S. *J. Am. Chem. Soc.* **2007**, *129*, 4512–4513. (g) Aitipamula, S.; Thallapally, P. K.; Thaimattam, R.; Jaskolski, M.; Desiraju, G. R. *Org. Lett.* **2002**, *4*, 921–924. (h) Sokolov, A. N.; MacGillivray, L. R. *Cryst. Growth Des.* **2006**, *6*, 2615–2624.
- (6) (a) Luan, X. J.; Wang, Y. Y.; Li, D. S.; Liu, P.; Hu, H. M.; Shi, Q. Z.; Peng, S. M. *Angew. Chem., Int. Ed.* **2005**, *44*, 3864–3867. (b) Luan, X. J.; Cai, X. H.; Wang, Y. Y.; Li, D. S.; Wang, C. J.; Liu, P.; Hu, H. M.; Shi, Q. Z.; Peng, S. M. *Chem. Eur. J.* **2006**, *12*, 6281–6289. (c) Yan, Q. Y.; Purkayastha, A.; Gandhi, D.; Li, H. F.; Kim, T.; Ramanath, G. *Adv. Mater.* **2007**, *19*, 3286–3290.
- (7) (a) Shorthill, B. J.; Avetta, C. T.; Glass, T. E. *J. Am. Chem. Soc.* **2004**, *126*, 12732–12733. (b) Zyryanov, G. V.; Rudkevich, D. M. *J. Am. Chem. Soc.* **2004**, *126*, 4264–4270. (c) Yang, E.; Zhang, J.; Li, Z. J.; Gao, S.; Kang, Y.; Chen, Y. B.; Wen, Y. H.; Yao, Y. G. *Inorg. Chem.* **2004**, *43*, 6525–6527.
- (8) (a) Lehn, J. M. *Supramolecular Chemistry: Concepts and Perspectives*; WHC: Weinheim, Germany, 1995. (b) Lehn, J. M.; Rigault, A.; Siegel, J.; Harrowfield, J.; Chevrier, B.; Moras, D. *Proc. Natl. Acad. Sci. U.S.A.* **1987**, *84*, 2565–2569. (c) Koert, M.; Harding, M.; Lehn, J. M. *Nature* **1990**, *346*, 339–342. (d) Berl, V.; Huc, I.; Khoury, R. G.; Krische, M. J.; Lehn, J. M.; Schmutz, R. *Nature* **2000**, *407*, 720–723. (e) Giuseppone, N.; Schmitt, J. L.; Lehn, J. M. *J. Am. Chem. Soc.* **2006**, *128*, 16748–16763. (f) Piguet, C.; Bernardinelli, G.; Hopfgartner, G. *Chem. Rev.* **1997**, *97*, 2005–2062. (g) Bünzli, J. C. G.; Piguet, C. *Chem. Rev.* **2002**, *102*, 1897–1928. (h) Albrecht, M. *Chem. Rev.* **2001**, *101*, 3457–3497. (i) Albrecht, M. *Angew. Chem., Int. Ed.* **2005**, *44*, 6448–6451. (j) Hill, D. J.; Mio, M. J.; Prince, R. B.; Hughes, T. S.; Moore, J. S. *Chem. Rev.* **2001**, *101*, 3893–4012. (k) Nakano, T.; Okamoto, Y. *Chem. Rev.* **2001**, *101*, 4013–4038. (l) Caulder, D. L.; Raymond, K. N. *Acc. Chem. Res.* **1999**, *32*, 975–982. (m) von Zelewsky, A. *Coord. Chem. Rev.* **1999**, *190*–192, 811–825. (n) Knof, U.; von Zelewsky, A. *Angew. Chem., Int. Ed.* **1999**, *38*, 302–322. (o) Rowan, A. E.; Nolte, R. J. M. *Angew. Chem., Int. Ed.* **1998**, *37*, 63–68.
- (9) (a) Zhang, Q.; Bu, X.; Lin, Z.; Biasini, M.; Beyermann, W. P.; Feng, P. *Inorg. Chem.* **2007**, *46*, 7262–7264. (b) Han, L.; Valle, H.; Bu, X. *Inorg. Chem.* **2007**, *46*, 1511–1513. (c) Tanaka, Y.; Katagiri, H.; Furusho, Y.; Yashima, E. *Angew. Chem., Int. Ed.* **2005**, *44*, 3867–3870. (d) Sugimoto, T.; Suzuki, T.; Shinkai, S.; Sada, K. *J. Am. Chem. Soc.* **2007**, *129*, 270–271. (e) Goto, H.; Katagiri, H.; Furusho, Y.; Yashima, E. *J. Am. Chem. Soc.* **2006**, *128*, 7176–7178. (f) Bae, J.; Choi, J. H.; Yoo, Y. S.; Oh, N. K.; Kim, B. S.; Lee, M. J. *J. Am. Chem. Soc.* **2005**, *127*, 9668–9669. (g) Green, M. M.; Park, J. W.; Sato, T.; Teramoto, A.; Lifson, S.; Selinger, R. L. B.; Selinger, J. V. *Angew. Chem., Int. Ed.* **1999**, *38*, 3138–3154.
- (10) (a) Zerkert, K.; Hamacek, J.; Senegas, J. M.; Dalla-Favera, N.; Floquet, S.; Bernardinelli, G.; Piguet, C. *Angew. Chem., Int. Ed.* **2005**, *44*, 7954–7958. (b) Matthews, C. J.; Onions, S. T.; Morata, G.; Davis, L. J.; Heath, S. L.; Price, D. J. *Angew. Chem., Int. Ed.* **2003**, *42*, 3166–3169. (c) Provent, C.; Hewage, S.; Brand, G.; Bernardinelli, G.; Charbonnière, L. J.; Williams, A. F. *Angew. Chem., Int. Ed.* **1997**, *36*, 1287–1289. (d) Albrecht, M.; Blau, O.; Fröhlich, R. *Proc. Natl. Acad. Sci. U.S.A.* **2002**, *99*, 4867–4872. (e) Jensen, T. B.; Scopelliti, R.; Bünzli, J. C. G. *Inorg. Chem.* **2006**, *45*, 7806–7814. (f) Grote, Z.; Bonazzi, S.; Scopelliti, R.; Severin, K. *J. Am. Chem. Soc.* **2006**, *128*, 10382–10383. (g) Elhabiri, M.; Hamacek, J.; Bünzli, J. C. G.; Albrecht-Gary, M. M. *Eur. J. Inorg. Chem.* **2004**, 51–62.
- (11) (a) Shieh, S. J.; Chou, C. C.; Lee, G. H.; Wang, C. F.; Peng, S. M. *Angew. Chem., Int. Ed.* **1997**, *109*, 57–59. (b) Cotton, F. A.; Daniels, L. M.; Jordan, G. T.; Murillo, C. A. *J. Am. Chem. Soc.* **1997**, *119*, 10377–10381. (c) Burkill, H. A.; Vilar, R.; White, A. J. P.; Williams, D. J. *J. Chem. Soc., Dalton Trans.* **2002**, 837–839. (d) Barbour, L. J.; Orr, G. W.; Atwood, J. L. *Nature* **1998**, *393*, 671–673. (e) McMorrán, D. A.; Steel, P. J. *Angew. Chem., Int. Ed.* **1998**, *37*, 3295–3297. (f) Xu, J. D.; Raymond, K. N. *Angew. Chem., Int. Ed.* **2006**, *45*, 6480–6485. (g) Bermejo, M. R.; González-Noya, A. M.; Pedrido, R. M.; Romero, M. J.; Vázquez, M. *Angew. Chem., Int. Ed.* **2005**, *44*, 4182–4187. (h) Cui, Y.; Lee, S. J.; Lin, W. B. *J. Am. Chem. Soc.* **2003**, *125*, 6014–6015. (i) Albrecht, M.; Witt, K.; Röttele, H.; Fröhlich, R. *Chem. Commun.* **2001**, 1330–1331.

like 4,4'-bipyridine, we have recently been interested in the assembly of cluster-based supramolecular compounds from M/Cu/S cluster precursors.<sup>20</sup> To date, most of these cluster-based compounds are of two- or three-dimensional frameworks, and only three compounds with 1D backbones have been isolated in the common chain forms such as zigzag,<sup>20e</sup> ladder,<sup>20c</sup> and single-stranded helix.<sup>20f</sup> Is it therefore possible

Chart 1. Possible Conformations of the bpe and bpp Ligands



- (12) Müller, A.; Diemann, E.; Jostes, R.; Bögge, H. *Angew. Chem., Int. Ed. Engl.* **1981**, *20*, 934–955. (b) Müller, A.; Bögge, H.; Schimanski, U.; Penk, M.; Nieradzki, K.; Dartmann, M.; Krickemeyer, E.; Schimanski, J.; Römer, C.; Römer, M.; Dornfeld, H.; Wienböcker, U.; Hellmann, W. *Monatsh. Chem.* **1989**, *120*, 367–391.
- (13) (a) Ansari, M. A.; Ibers, J. A. *Coord. Chem. Rev.* **1990**, *100*, 223–266. (b) Jeannin, Y.; Séheresse, F.; Bernés, S.; Robert, F. *Inorg. Chim. Acta* **1992**, *198–200*, 493–505.
- (14) (a) Wu, X. T.; Chen, P. C.; Du, S. W.; Zhu, N. Y.; Lu, J. X. *J. Cluster Sci.* **1994**, *5*, 265–285. (b) Wu, X. T. *Inorganic Assembly Chemistry*; Science Press: Beijing, China, 2004; pp 1–179. (c) Zhang, W. J.; Behrens, A.; Gätjens, J.; Ebel, M.; Wu, X. T.; Rehder, D. *Inorg. Chem.* **2004**, *43*, 3020–3023. (d) Song, L.; Li, J. R.; Lin, P.; Li, Z. H.; Li, T.; Du, S. W.; Wu, X. T. *Inorg. Chem.* **2006**, *45*, 10155–10161.
- (15) (a) Chan, C. K.; Guo, C. X.; Wang, R. J.; Mak, T. C. W.; Che, C. M. *J. Chem. Soc., Dalton Trans.* **1995**, 753–757. (b) Che, C. M.; Xia, B. H.; Huang, J. S.; Chan, C. K.; Zhou, Z. Y.; Cheung, K. K. *Chem. Eur. J.* **2001**, *7*, 3998–4006.
- (16) (a) Wu, D. X.; Hong, M. C.; Cao, R.; Liu, H. Q. *Inorg. Chem.* **1996**, *35*, 1080–1082. (b) Hou, H. W.; Xin, X. Q.; Shi, S. *Coord. Chem. Rev.* **1996**, *153*, 25–56. (c) Zhang, Q. F.; Niu, Y. Y.; Lueng, W. H.; Song, Y. L.; Williams, I. D.; Xin, X. Q. *Chem. Commun.* **2001**, 1126–1127. (d) Arikawa, Y.; Kawaguchi, H.; Kashiwabara, K.; Tatsumi, K. *Inorg. Chem.* **2002**, *41*, 513–520. (e) Niu, Y. Y.; Zheng, H. G.; Xin, X. Q. *Coord. Chem. Rev.* **2004**, *248*, 169–183. (f) Liang, K.; Zheng, H. G.; Song, Y. L.; Li, Y. Z.; Xin, X. Q. *Cryst. Growth Des.* **2007**, *7*, 373–376. (g) Zhang, J. F.; Song, Y. L.; Yang, J. Y.; Humphery, M. G.; Zhang, C. *Cryst. Growth Des.* **2008**, *8*, 387–390.
- (17) (a) Shi, S.; Ji, W.; Tang, S. H.; Lang, J. P.; Xin, X. Q. *J. Am. Chem. Soc.* **1994**, *116*, 3615–3616. (b) Lang, J. P.; Xin, X. Q. *J. Solid State Chem.* **1994**, *108*, 118–127. (c) Shi, S.; Ji, W.; Lang, J. P.; Xin, X. Q. *J. Phys. Chem.* **1994**, *98*, 3570–3572. (d) Shi, S.; Ji, W.; Xie, W.; Chong, T. C.; Zheng, H. C.; Lang, J. P.; Xin, X. Q. *Mater. Chem. Phys.* **1995**, *39*, 298–301.
- (18) (a) Lang, J. P.; Kawaguchi, H.; Ohnishi, S.; Tatsumi, K. *Chem. Commun.* **1997**, 405–406. (b) Lang, J. P.; Tatsumi, K. *Inorg. Chem.* **1998**, *37*, 160–162. (c) Lang, J. P.; Tatsumi, K. *Inorg. Chem.* **1998**, *37*, 6308–6316. (d) Lang, J. P.; Kawaguchi, H.; Ohnishi, S.; Tatsumi, K. *Inorg. Chim. Acta* **1998**, *283*, 136–144. (e) Yu, H.; Xu, Q. F.; Sun, Z. R.; Ji, S. J.; Chen, J. X.; Liu, Q.; Lang, J. P.; Tatsumi, K. *Chem. Commun.* **2001**, 2614–2615. (f) Lang, J. P.; Ji, S. J.; Xu, Q. F.; Shen, Q.; Tatsumi, K. *Coord. Chem. Rev.* **2003**, *241*, 47–60.
- (19) (a) Ren, Z. G.; Li, H. X.; Liu, G. F.; Zhang, W. H.; Lang, J. P.; Zhang, Y.; Song, Y. L. *Organometallics* **2006**, *25*, 4351–4357. (b) Yang, J. Y.; Gu, J. H.; Song, Y. L.; Shi, G.; Wang, Y. X.; Zhang, W. H.; Lang, J. P. *J. Phys. Chem. B* **2007**, *111*, 7987–7993. (c) Wang, J.; Sun, Z. R.; Deng, L.; Wei, Z. H.; Zhang, W. H.; Zhang, Y.; Lang, J. P. *Inorg. Chem.* **2007**, *46*, 11381–11389.
- (20) (a) Lang, J. P.; Kawaguchi, H.; Tatsumi, K. *Chem. Commun.* **1999**, 2315–2316. (b) Lang, J. P.; Xu, Q. F.; Chen, Z. N.; Abrahams, B. F. *J. Am. Chem. Soc.* **2003**, *125*, 12682–12683. (c) Lang, J. P.; Xu, Q. F.; Yuan, R. X.; Abrahams, B. F. *Angew. Chem., Int. Ed.* **2004**, *43*, 4741–4745. (d) Lang, J. P.; Jiao, C. M.; Qiao, S. B.; Zhang, W. H.; Abrahams, B. F. *Inorg. Chem.* **2005**, *44*, 3664–3668. (e) Xu, Q. F.; Chen, J. X.; Zhang, W. H.; Ren, Z. G.; Li, H. X.; Zhang, Y.; Lang, J. P. *Inorg. Chem.* **2006**, *45*, 4055–4064. (f) Lang, J. P.; Xu, Q. F.; Zhang, W. H.; Li, H. X.; Ren, Z. G.; Chen, J. X.; Zhang, Y. *Inorg. Chem.* **2006**, *45*, 10487–10496. (g) Zhang, W. H.; Song, Y. L.; Ren, Z. G.; Li, H. X.; Li, L. L.; Zhang, Y.; Lang, J. P. *Inorg. Chem.* **2007**, *46*, 6647–6660. (h) Ding, N. N.; Zhang, W. H.; Li, H. X.; Ren, Z. G.; Lang, J. P.; Zhang, Y.; Abrahams, B. F. *Inorg. Chem. Commun.* **2007**, *10*, 623–626. (i) Zhang, W. H.; Song, Y. L.; Zhang, Y.; Lang, J. P. *Cryst. Growth Des.* **2008**, *8*, 253–258. (j) Zhang, W. H.; Lang, J. P.; Zhang, Y.; Abrahams, B. F. *Cryst. Growth Des.* **2008**, *8*, 399–401.
- (21) (a) Holm, R. H. *Adv. Inorg. Chem.* **1992**, *38*, 1–71. (b) *Molybdenum Enzymes, Cofactors and Model Systems*; Stiefel, E. I., Coucouvanis, D., Newton, W. E., Eds.; ACS Symposium Series 535; American Chemical Society: Washington, DC, 1993. (c) *Transition Metal Sulfur Chemistry, Biological and Industrial Significance*; Stiefel, E. I., Matsumoto, K., Eds.; ACS Symposium Series 653; American Chemical Society: Washington, DC, 1996.

to make one-dimensional cluster-based chains with other single-, double-, triple-, and multiple-stranded forms? In our last report,<sup>20g</sup> we noticed that utilization of the low symmetrical ligand ( $C_2$  symmetry), 1,2-bis(4-pyridyl)ethane (bpe) (Chart 1), could induce the bulky  $\eta^5$ - $C_5Me_5$ -coordinated  $[MoS_3Cu_3]$  core to form irregular topological nodes, which resulted in the formation of a less symmetrical structure of  $\{[(\eta^5-C_5Me_5)MoS_3Cu_3]_2(NCS)_3(\mu-NCS)(bpe)_3\} \cdot 3aniline\}_n$ . This 2D structure may be viewed as being built of one-dimensional zigzag chains  $\{[(\eta^5-C_5Me_5)MoS_3Cu_3]_2(\mu-bpe)_6(NCS)_6\}_n$  linked by double thiocyanate bridges. If such thiocyanate bridges could be prevented, there might be a chance to create a compound with the desired 1D zigzag chain. Considering that the thiocyanate bridges are formed between two bulky  $[(\eta^5-C_5Me_5)MoS_3Cu_3]$  cores, replacement of the thiocyanate bridges with shorter bromide bridges may cause higher steric hindrance between the two cluster cores, which may in turn break up such Br bridges, forming 1D chain structures. In this regard,  $[PPh_4][(\eta^5-C_5Me_5)MoS_3(CuBr)_3]$  (**1a**)<sup>18a</sup> along with bpe was selected for this proposal. Fortunately, reactions of **1a** with bpe through controlling their molar ratios produced five interesting cluster-based compounds **2–5** (Chart 2). In these structures, the  $[(\eta^5-C_5Me_5)MoS_3Cu_3]$  core under the presence of the bridging ligand bpe works as various multiconnecting nodes to form four different 1D chain arrays (Scheme 1). For comparative studies, another low symmetrical ligand 1,3-bis(4-pyridyl)propane (bpp) (Chart 1) was used to react with **1a** and its thiocyanate analogue  $[PPh_4][(\eta^5-C_5Me_5)MoS_3Cu_3(NCS)_3]$  (**1b**), thereby

- (22) (a) George, G. N.; Pickering, I. J.; Yu, Y. E.; Prince, R. C.; Bursakov, S. A.; Gavel, O. Y.; Moura, I.; Moura, J. J. G. *J. Am. Chem. Soc.* **2000**, *122*, 8321–8322. (b) Dobbek, H.; Gremer, L.; Kiefersauer, R.; Huber, R.; Meyer, O. *Proc. Natl. Acad. Sci. U.S.A.* **2002**, *99*, 15971–15976. (c) Ginda, M.; Ferner, R.; Gremer, L.; Meyer, O.; Meyer-Klaucke, W. *Biochemistry* **2003**, *42*, 222–230. (d) George, G. N.; Pickering, I. J.; Harris, H. H.; Gailer, J.; Klein, D.; Lichtmannegger, J.; Summer, K. H. *J. Am. Chem. Soc.* **2003**, *125*, 1704–1705. (e) Takuma, M.; Ohki, Y.; Tatsumi, K. *Inorg. Chem.* **2005**, *44*, 6034–6043.
- (23) Shi, S. In *Optoelectronic Properties of Inorganic Compounds*; Roundhill, D. M., Fackler, J. P., Jr., Eds.; Plenum: New York, 1998; pp 55–105. (b) Coe, B. J. In *Comprehensive Coordination Chemistry II*; McCleverty, J. A., Meyer, T. J., Eds.; Elsevier: Oxford, U.K., 2004; Vol. 9, pp 621–687.
- (24) (a) Zheng, H. G.; Ji, W.; Low, M. L. K.; Sakane, G.; Shibahara, T.; Xin, X. Q. *J. Chem. Soc., Dalton Trans.* **1997**, 2375–2362. (b) Hou, H. W.; Zheng, H. G.; Ang, H. G.; Fan, Y. T.; Low, M. L. K.; Zhu, Y.; Wang, W. L.; Xin, X. Q.; Ji, W.; Wong, W. T. *J. Chem. Soc., Dalton Trans.* **1999**, 2953–2957. (c) Zhang, C.; Song, Y. L.; Xu, Y.; Fun, H. K.; Fang, G. Y.; Wang, Y. X.; Xin, X. Q. *J. Chem. Soc., Dalton Trans.* **2000**, 2823–2829. (d) Zhang, C.; Song, Y. L.; Wang, X. *Coord. Chem. Rev.* **2007**, *251*, 111–141.

**Chart 2.** Designation of Compounds and Abbreviations<sup>a</sup> for 1–7

 $[\text{PPh}_4][(\eta^5\text{-C}_5\text{Me}_5)\text{MoS}_3(\text{CuX})_3]$  (**1a**: X = Br,<sup>18a</sup> **1b** = NCS<sup>20g</sup>)

 $\{[(\eta^5\text{-C}_5\text{Me}_5)\text{MoS}_3\text{Cu}_3]_2(\mu\text{-bpe})_{3.5}\text{Br}_4\cdot\text{MeCN}\}_n$  (**2**),

 $\{[(\eta^5\text{-C}_5\text{Me}_5)\text{MoS}_3\text{Cu}_3]_2(\mu\text{-bpe})_3\text{Br}_4\cdot\text{DMSO}\cdot 3\text{MeCN}\}_n$  (**3a**)

 $\{[(\eta^5\text{-C}_5\text{Me}_5)\text{MoS}_3\text{Cu}_3]_2(\mu\text{-bpe})_3\text{Br}_4\cdot 2\text{aniline}\cdot 3\text{MeCN}\}_n$  (**3b**)

 $\{[(\eta^5\text{-C}_5\text{Me}_5)\text{MoS}_3\text{Cu}_3]_2(\mu\text{-bpe})_3(\text{bpe})\text{Br}_4\cdot 0.35\text{DMF}\}_n$  (**4**)

 $\{[(\eta^5\text{-C}_5\text{Me}_5)\text{MoS}_3\text{Cu}_3]_2(\mu\text{-bpe})_2(\mu\text{-Br})(\mu_3\text{-Br})\text{Br}_2\cdot\text{DMF}\cdot\text{MeCN}\}_n$  (**5**)

 $(\eta^5\text{-C}_5\text{Me}_5)\text{MoS}_3\text{Cu}_3(\mu\text{-bpp})(\mu\text{-Br})\text{Br}_n$  (**6**)

 $\{[(\eta^5\text{-C}_5\text{Me}_5)\text{MoS}_3\text{Cu}_3]_2(\mu\text{-bpp})_2(\mu\text{-NCS})_2(\text{NCS})\}_n$  (**7**)

<sup>a</sup> bpe = 1,2-bis(4-pyridyl)ethane; bpp = 1,3-bis(4-pyridyl)propane.

resulting in the isolation of two more cluster-supported compounds with rare 1D triply stranded and quadruply stranded chains **6** and **7** (Chart 2 and Scheme 1). In this paper, we report their assembly reactions, crystal structures, and third-order nonlinear optical properties in aniline.

## Results and Discussion

**Synthetic and Spectral Aspects.** Reactions of **1a** with bpe in a molar ratio of 2:3.5 in DMF/MeCN followed by a standard workup gave rise to **2** as black prisms in 70% yield, while those of **1a** with bpe (molar ratio = 2:3) in DMSO/MeCN afforded black needles of **3a** in 76% yield. The differences between the two reactions are the cluster-to-ligand ratio and the solvent system. Therefore, which one plays the critical role in the formation of these cluster-based assemblies? We first examined the solvent systems. Reaction of **1a** with bpe (molar ratio = 2:3) in aniline/MeCN followed by a similar workup produced black plates of **3b** in 72% yield. As discussed later in this paper, **3a** is isostructural to **3b**, though the former holds DMSO and MeCN solvent molecules while the latter has aniline and MeCN solvent molecules in their crystals. This result suggests that there is no solvent effect in these cases. Then, we explored the cluster-to-ligand stoichiometries. Reactions of **1a** and 2 equiv of bpe in DMF/MeCN gave rise to black square thin plates of **4** in 48% yield accompanied with some black prisms of **2**. Efforts made to ensure the formation of **4** in pure form proved to be unsuccessful, although several reactions with different molar ratios of **1a** and bpe around 1:3–1:4 were carried out. When the **1a**-to-bpe molar ratio became 1:1, similar reactions of **1a** with bpe in DMF/MeCN led to the formation of black plates of **5** in 78% yield. The 2:1 (or 3:1) mixture of **1a** and bpe in DMF/MeCN always gave a mixture of **5** and unreacted **1a**. According to the subsequent X-ray analysis of **2–5**, their structures contain the corresponding  $[(\eta^5\text{-C}_5\text{Me}_5)\text{MoS}_3\text{Cu}_3]/\text{bpe}$  ratios of 2:3.5 for **2**, 2:3 for **3**, 1:2 for **4**, and 1:1 for **5**, which are consistent with the **1a**-to-ligand ratio used in the initial assembly reactions. In this regard, the different outcomes of the reactions of **1a** with bpe in DMF/MeCN are suggested to be highly dependent

on the stoichiometric ratio of **1a**/bpe. To our knowledge, the formation of four different kinds of cluster-based complexes with various 1D chain structures from reactions of the same components with different cluster-to-ligand ratios is unprecedented.

Intriguingly, when we explored the assembly reactions of **1a** and **1b** with a more flexible ligand bpp, they produced two more complicated cluster-based complexes. Reactions of a solution of **1a** in DMF with 1.5 equiv of bpp in MeCN followed by a similar workup to that used in the isolation of **2** afforded black block crystals of **6** (64% yield), which, according to the X-ray analysis described in this paper, contains a  $[(\eta^5\text{-C}_5\text{Me}_5)\text{MoS}_3\text{Cu}_3]/\text{bpp}$  ratio of 1:1 in its structure. However, analogous reactions of **1b** and bpp (molar ratio = 1:1.5) in the same solvent system produced black plates of **7** in 78% yield. Compound **7** has the correct 1:1.5  $[(\eta^5\text{-C}_5\text{Me}_5)\text{MoS}_3\text{Cu}_3]/\text{bpp}$  ratio in its structure. Parallel reactions using different cluster-to-ligand ratios and different solvent systems such as DMSO and aniline did not form the expected cluster-based polydimensional complexes with different  $[(\eta^5\text{-C}_5\text{Me}_5)\text{MoS}_3\text{Cu}_3]/\text{bpp}$  ratios but always produced **6** or **7** in 20–50% yields. These results suggest that the formation of **6** or **7** may depend neither on the **1a** (**1b**)/bpp ratio nor solvent effects.

Solids **2–7** were relatively stable toward air and moisture. They were insoluble in common solvents such as MeCN,  $\text{CH}_2\text{Cl}_2$ , and  $\text{CHCl}_3$ , slightly soluble in DMF and DMSO, but readily soluble in aniline. The elemental analyses were consistent with their chemical formulas. In the IR spectra of **2–7**, bands at 414 (**2**), 409 (**3a**), 411 (**3b**), 412 (**4**), 414 (**5**), 415 (**6**), and 408 (**7**)  $\text{cm}^{-1}$  were assigned as the bridging Mo–S stretching vibrations. In **7**, one broad band at 2079  $\text{cm}^{-1}$  may be assigned to be an overlapped signal by the stretching vibrations of the free NCS and the terminal NCS groups. The band at 2101  $\text{cm}^{-1}$  was assigned as the bridging NCS stretching vibration. The  $^1\text{H}$  NMR spectra in  $\text{DMSO-}d_6$  at ambient temperature showed a sharp singlet of  $\eta^5\text{-C}_5\text{Me}_5$  at 1.97 (**2**), 1.96 (**3a**), 2.01 (**3b**), 1.96 (**4**), 1.95 (**5**), 1.92 (**6**), and 1.90 (**7**) ppm. Other resonances in their  $^1\text{H}$  NMR spectra were assigned as follows: multiplets in the ranges 7.43–8.62 (**2**), 7.36–8.59 (**3a**), 7.24–8.45 (**3b**), 7.40–8.54 (**4**), 7.38–8.45 (**5**), 6.55–7.26 (**6**), and 7.70–7.98 (**7**) ppm for pyridyl protons, singlets at 3.05 (**2**), 3.01 (**3a**), 3.03 (**3b**), 3.06 (**4**), and 3.04 (**5**) ppm for methylene protons of bpe, and multiplets in the regions 2.06–2.66 (**6**) and 2.01–2.59 (**7**) ppm for methylene protons of bpp, respectively. The identities of **2–7** were further confirmed by X-ray crystallography.

**Crystal Structure of  $\{[(\eta^5\text{-C}_5\text{Me}_5)\text{MoS}_3\text{Cu}_3]_2(\mu\text{-bpe})_{3.5}\text{Br}_4\cdot\text{MeCN}\}_n$  (**2**).** Compound **2** crystallizes in the monoclinic space group  $P2_1/c$ , and each asymmetric unit contains half of a  $\{[(\eta^5\text{-C}_5\text{Me}_5)\text{MoS}_3\text{Cu}_3]_2(\mu\text{-bpe})_7\text{Br}_8\}$  molecule and one MeCN solvent molecule. As shown in Figure 1, this molecule consists of two different dimeric units,  $\{[(\eta^5\text{-C}_5\text{Me}_5)\text{MoS}_3\text{Cu}_3]_2(\mu\text{-bpe})_4\text{Br}_4\}$  (unit A) and  $\{[(\eta^5\text{-C}_5\text{Me}_5)\text{MoS}_3\text{Cu}_3]_2(\mu\text{-bpe})_3\text{Br}_4\}$  (unit B), which are interconnected by a pair of bridging bpe ligands. Unit A and unit B assume two different double incomplete cubane-like structures. For unit A, two single incomplete cubane-like  $[(\eta^5\text{-C}_5\text{Me}_5)\text{MoS}_3\text{Cu}_3(\text{bpe})_2\text{Br}_2]$  fragments are linked by a pair

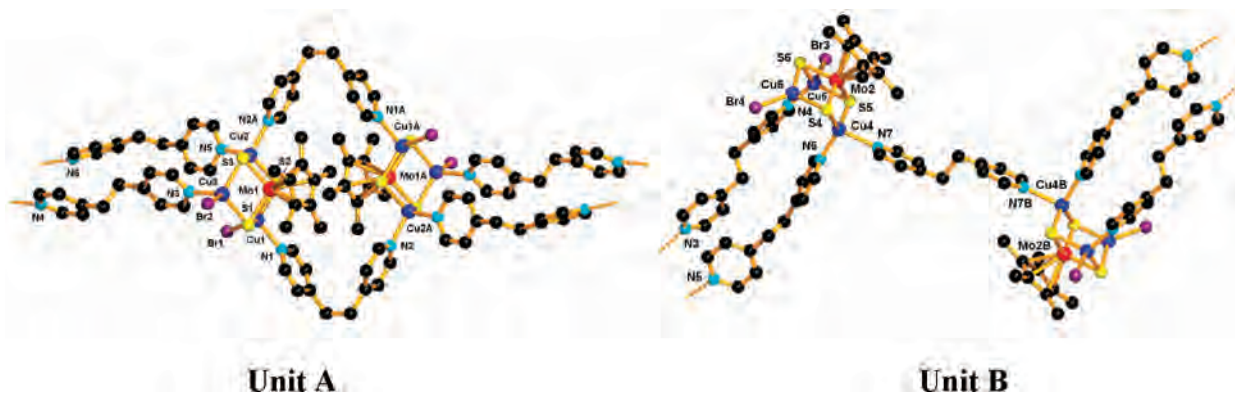
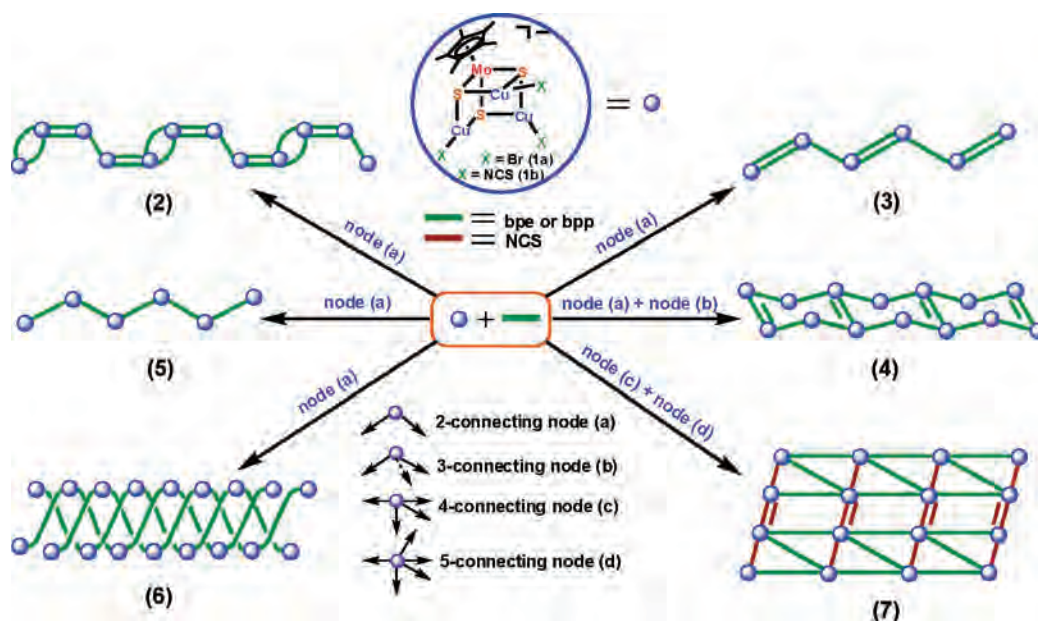


**Figure 1.** Perspective view of the dimeric  $[(\eta^5\text{-C}_5\text{Me}_5)\text{MoS}_3\text{Cu}_3]_2(\mu\text{-bpe})_6\text{Br}_4$  unit (unit A) in **2** with labeling scheme (left). Perspective view of the dimeric  $[(\eta^5\text{-C}_5\text{Me}_5)\text{MoS}_3\text{Cu}_3]_2(\mu\text{-bpe})_5\text{Br}_4$  unit (unit B) in **2** with labeling scheme (right). All the hydrogen atoms along with the disordered non-hydrogen atoms were omitted for clarity. Symmetry codes: (A)  $-x + 1, -y, -z + 1$ ; (B)  $-x - 1, -y, -z$ .

**Scheme 1.** Possible Topological Nodes and Frameworks Derived from **1** and bpe or bpp Ligands



of bridging bpe ligands (Figure 1, left), while those in unit B are connected by a single bridging bpe ligand (Figure 1, right). There is a crystallographic inversion center located at the midpoint of the Mo1 and Mo1A contact (unit A) or the Mo2 and Mo2B separation (unit B).

Although each fragment of **2** assumes the incomplete cubane-like  $[(\eta^5\text{-C}_5\text{Me}_5)\text{MoS}_3\text{Cu}_3]$  core structure of **1a**, the three copper atoms in each fragment have different coordination geometries from those of **1a**. In unit A, three Cu centers adopt distorted tetrahedral coordination geometries. By being coordinated by two  $\mu_3\text{-S}$  atoms from the  $[(\eta^5\text{-C}_5\text{Me}_5)\text{MoS}_3]$  moiety, Cu1 or Cu3 is coordinated by one terminal Br and one bridging bpe ligand, while Cu2 is coordinated by two bridging bpe ligands. The mean Mo1...Cu contact (2.693(3) Å) (Table 1) is slightly longer than those of the clusters containing tetrahedrally coordinated Cu such as  $\{[\text{MoOS}_3\text{Cu}_3\text{I}(\text{dpds})_2] \cdot 0.5\text{DMF} \cdot 2(\text{MeCN})_{0.5}\}_n$  (avg 2.6820(15) Å) and  $\{[\text{MoOS}_3\text{Cu}_3(\text{dca})(4,4'\text{-bipy})_{1.5}] \cdot \text{DMF} \cdot \text{MeCN}\}_n$  (avg 2.6782(12) Å).<sup>20f</sup> In unit B, the three Cu atoms in each fragment have either a trigonal planar or a tetrahedral coordination geometry. By being coordinated by two  $\mu_3\text{-S}$  atoms from the  $[(\eta^5\text{-C}_5\text{Me}_5)\text{MoS}_3]$  moiety, Cu4 is coordi-

nated by two bridging bpe ligands, Cu5 by a terminal Br and a bridging bpe ligand, and Cu6 by only a terminal Br. For the tetrahedrally coordinated Cu4 and Cu5, the mean Mo2...Cu contact (2.696(3) Å) is quite close to that of unit A, while for the trigonally coordinated Cu6, the Mo2...Cu6 separation (2.619(3) Å) is slightly shorter than that of **1**. Interestingly, the bpe ligands in unit A show a *gauche-gauche* conformation while those in unit B have a *trans-trans* conformation. The mean Cu-N(bpe) length (2.092 Å) in **2** is longer than that observed in  $\{[(\eta^5\text{-C}_5\text{Me}_5)\text{WS}_3\text{Cu}_3\text{Cl}(\text{MeCN})(1,4\text{-pyz})](\text{PF}_6)_n\}$  (1.975(1) Å).<sup>20a</sup> The mean Mo- $\mu_3\text{-S}$ , Cu- $\mu_3\text{-S}$  and the terminal Cu-Br bond lengths are similar to those of the corresponding ones of  $[\text{PPh}_4]_2[\text{MoS}_4\text{Cu}_4\text{Br}_4]$ ,<sup>25</sup>  $[\text{Et}_4\text{N}]_2[\text{MoOS}_3\text{Cu}_3\text{I}_2\text{Br}]$ ,<sup>26</sup> and **1a**.

Topologically, each  $[(\eta^5\text{-C}_5\text{Me}_5)\text{MoS}_3\text{Cu}_3]$  core in unit A and unit B serves as an angular two-connecting node. Two such nodes interconnect through pairs of bpe bridges to form a  $[(\eta^5\text{-C}_5\text{Me}_5)\text{MoS}_3\text{Cu}_3]_2(\text{bpe})_2\text{Br}_4$  unit. Furthermore, this

(25) Nicholson, J. R.; Flood, A. C.; Garner, C. D.; Clegg, W. *Chem. Commun.* **1983**, 1179–1180.

(26) Hou, H. W.; Xin, X. Q.; Liu, J.; Chen, M. Q.; Shi, S. *J. Chem. Soc., Dalton Trans.* **1994**, 3211–3214.

**Table 1.** Selected Bond Distances (Å) and Angles (deg) for **2**

Mo(1)···Cu(1)	2.707(3)	Mo(1)···Cu(2)	2.685(3)
Mo(1)···Cu(3)	2.689(3)	Mo(2)···Cu(4)	2.680(3)
Mo(2)···Cu(5)	2.713(3)	Mo(2)···Cu(6)	2.619(3)
Mo(1)–S(1)	2.279(5)	Mo(1)–S(3)	2.285(5)
Mo(1)–S(2)	2.286(4)	Mo(2)–S(5)	2.256(5)
Mo(2)–S(6)	2.288(5)	Mo(2)–S(4)	2.294(6)
Cu(1)–N(1)	2.152(15)	Cu(1)–S(1)	2.241(5)
Cu(1)–S(2)	2.247(5)	Cu(1)–Br(1)	2.402(3)
Cu(2)–N(5)	2.014(18)	Cu(2)–N(2A)	2.136(15)
Cu(2)–S(3)	2.234(5)	Cu(2)–S(2)	2.242(5)
Cu(3)–N(3)	2.049(14)	Cu(3)–S(3)	2.227(5)
Cu(3)–S(1)	2.230(5)	Cu(3)–Br(2)	2.460(4)
Cu(4)–N(6)	2.062(16)	Cu(4)–S(5)	2.213(6)
Cu(4)–S(4)	2.232(6)	Cu(4)–N(7)	2.338(8)
Cu(5)–N(4)	2.028(15)	Cu(5)–S(6)	2.241(6)
Cu(5)–S(5)	2.250(6)	Cu(5)–Br(3)	2.454(3)
Cu(6)–S(6)	2.198(6)	Cu(6)–S(4)	2.208(6)
Cu(6)–Br(4)	2.265(4)		
S(1)–Mo(1)–S(3)	104.98(17)	S(1)–Mo(1)–S(2)	105.21(17)
S(3)–Mo(1)–S(2)	105.58(17)	S(5)–Mo(2)–S(6)	105.28(19)
S(5)–Mo(2)–S(4)	105.0(2)	S(6)–Mo(2)–S(4)	105.5(2)
N(1)–Cu(1)–S(1)	106.0(5)	N(1)–Cu(1)–S(2)	108.1(5)
N(1)–Cu(1)–S(2)	107.83(18)	N(1)–Cu(1)–Br(1)	92.7(4)
S(1)–Cu(1)–Br(1)	121.08(16)	S(2)–Cu(1)–Br(1)	118.37(16)
N(5)–Cu(2)–N(2A)	96.4(10)	N(5)–Cu(2)–S(3)	119.4(8)
N(2A)–Cu(2)–S(3)	107.7(5)	N(5)–Cu(2)–S(2)	116.7(9)
N(2A)–Cu(2)–S(2)	105.7(4)	S(3)–Cu(2)–S(2)	108.82(18)
N(3)–Cu(3)–S(3)	109.2(4)	S(1)–Cu(3)–Br(2)	106.06(17)
N(3)–Cu(3)–S(1)	118.3(5)	S(3)–Cu(3)–S(1)	108.63(18)
N(3)–Cu(3)–Br(2)	100.3(4)	S(3)–Cu(3)–Br(2)	114.39(16)
N(6)–Cu(4)–S(5)	118.1(8)	S(4)–Cu(4)–N(7)	116.3(3)
N(6)–Cu(4)–S(4)	119.4(8)	S(5)–Cu(4)–S(4)	108.6(2)
N(6)–Cu(4)–N(7)	96.8(8)	S(5)–Cu(4)–N(7)	94.5(3)
N(4)–Cu(5)–S(6)	111.6(5)	S(5)–Cu(5)–Br(3)	103.10(18)
N(4)–Cu(5)–S(5)	117.1(5)	S(6)–Cu(5)–S(5)	107.1(2)
N(4)–Cu(5)–Br(3)	100.5(5)	S(6)–Cu(5)–Br(3)	117.59(19)
S(6)–Cu(6)–Br(4)	126.2(2)	S(4)–Cu(6)–Br(4)	122.1(2)
S(6)–Cu(6)–S(4)	111.7(2)		

unit links the equivalent units alternatively by double bpe bridges and single bpe bridges to form a 1D “Great Wall”-like chain (parallel to the [101] direction) (Figure 2). The 1D chains are closely packed in the unit cell as a result of a variety of intermolecular interactions such as hydrogen bonding and  $\pi$ – $\pi$  interactions. The MeCN solvent molecules are deeply buried in the lattice, and each is fitted in a small chamber enclosed by neighboring chains (see the Supporting Information).

**Crystal Structures of  $\{[(\eta^5\text{-C}_5\text{Me}_5)\text{MoS}_3\text{Cu}_3]_2(\mu\text{-bpe})_3\text{Br}_4\}\cdot\text{Sol}_n$  (**3a**: Sol = DMSO·3MeCN; **3b**: Sol = 2aniline·3MeCN).** Because they have a common chemical formula  $\{[(\eta^5\text{-C}_5\text{Me}_5)\text{MoS}_3\text{Cu}_3]_2(\mu\text{-bpe})_3\text{Br}_4\}\cdot\text{Sol}_n$ , **3a** and **3b** both crystallize in the triclinic space group  $P\bar{1}$ , and the asymmetric unit contains half of a  $\{[(\eta^5\text{-C}_5\text{Me}_5)\text{MoS}_3\text{Cu}_3]_2(\mu\text{-bpe})_3\text{Br}_4\}$  molecule, half of a DMSO molecule, and one and a half MeCN solvent molecules (**3a**) or one discrete  $\{[(\eta^5\text{-C}_5\text{Me}_5)\text{MoS}_3\text{Cu}_3]_2(\mu\text{-bpe})_3\text{Br}_4\}$  molecule, two aniline molecules, and three MeCN solvent molecules (**3b**). Their cell parameters are essentially identical, as are their structures. Therefore, only the structure of **3a** is shown in Figure 3. Only the pertinent bond lengths and angles for **3a** are listed in Table 2. The  $\{[(\eta^5\text{-C}_5\text{Me}_5)\text{MoS}_3\text{Cu}_3]_2(\mu\text{-bpe})_3\text{Br}_4\}$  molecule in **3a** or **3b** consists of two incomplete cubane-like  $[(\eta^5\text{-C}_5\text{Me}_5)\text{MoS}_3\text{Cu}_3(\mu\text{-bpe})_{0.5}\text{Br}_2]$  fragments linked by a single bpe bridge, forming a double incomplete cubane-like structure similar

to that of unit B in **2**. Each  $[(\eta^5\text{-C}_5\text{Me}_5)\text{MoS}_3\text{Cu}_3(\mu\text{-bpe})_{0.5}\text{Br}_2]$  fragment retains the core structure of **1a**. Upon being coordinated by two  $\mu_3$ -S atoms from the  $[(\eta^5\text{-C}_5\text{Me}_5)\text{MoS}_3]$  moiety for each Cu atom, Cu1 is further coordinated by a terminal Br atom to give a trigonal planar coordination geometry while the other two Cu atoms are coordinated by two N atoms of two bpe ligands (Cu2) or by one terminal Br atom and one N atom of bpe (Cu3), forming a distorted tetrahedral geometry. The bpe ligands in **3a** or **3b** present as a *trans*–*trans* conformation. For the trigonally coordinated Cu1 and the tetrahedrally coordinated Cu2 and Cu3, the mean Mo1···Cu contacts (2.6163(16) vs 2.6858(15) Å for **3a** and 2.6326(12) vs 2.6898(10) Å for **3b**) are comparable to those of the corresponding ones of **2**. The average Mo– $\mu_3$ -S, Cu– $\mu_3$ -S, Cu–N, and terminal Cu–Br distances are normal.

Topologically, each  $[(\eta^5\text{-C}_5\text{Me}_5)\text{MoS}_3\text{Cu}_3]$  core in **3a** or **3b** acts as an angular two-connecting node (node (a)) to connect with its adjacent ones alternatively through single bpe bridges and double bpe bridges, forming a one-dimensional zigzag chain extended along the [101] axis. This chain holds the neighboring ones through intermolecular hydrogen-bonding interactions and  $\pi$ – $\pi$  interactions to give a 2D layer extending along the *ac* plane. The layer-to-layer separation is approximately 9.23 Å, and the DMSO and MeCN solvents are squeezed between the 2D layers (see the Supporting Information).

**Crystal Structure of  $\{[(\eta^5\text{-C}_5\text{Me}_5)\text{MoS}_3\text{Cu}_3]_2(\mu\text{-bpe})_3(\text{bpe})\text{Br}_4\}\cdot 0.35\text{DMF}_n$  (**4**).** Compound **4** crystallizes in the triclinic space group  $P\bar{1}$ , and the asymmetric unit contains one neutral  $\{[(\eta^5\text{-C}_5\text{Me}_5)\text{MoS}_3\text{Cu}_3]_2(\mu\text{-bpe})_3(\text{bpe})\text{Br}_4\}$  molecule. As shown in Figure 4, this molecule may be viewed as another kind of double incomplete cubane-like structure in which two different single incomplete cubane-like  $[(\eta^5\text{-C}_5\text{Me}_5)\text{MoS}_3\text{Cu}_3(\mu\text{-bpe})_{0.5}(\text{bpe})\text{Br}_2]$  and  $[(\eta^5\text{-C}_5\text{Me}_5)\text{MoS}_3\text{Cu}_3(\mu\text{-bpe})_{1.5}\text{Br}_2]$  fragments are linked by a single bridging bpe. The geometries of the MoS<sub>3</sub>Cu<sub>3</sub> cubes in both fragments are similar to those found in **1**–**3**. Among these two cluster fragments, there are six unique Cu centers, which can be divided into four different categories depending on their coordination environments. Upon being coordinated by two  $\mu_3$ -S atoms from the  $[(\eta^5\text{-C}_5\text{Me}_5)\text{MoS}_3]$  moiety, Cu1, Cu4, and Cu6 are coordinated by one N atom of one bridging bpe ligand and one terminal Br, Cu2 is coordinated by two N atoms of one bridging and one monocoordinated bpe ligands, and Cu5 is coordinated by two N atoms of two bridging bpe ligands, forming a distorted tetrahedral geometry, while Cu3 is coordinated only by one terminal Br to give a trigonal planar geometry. It is quite rare that one bpe (bearing N1 and N2) serves as a monocoordinated ligand, despite the fact that Cu3 still has one free site available for the further coordination by bpe ligands. As shown in Table 3, for the trigonally coordinated Cu3 and the tetrahedrally coordinated Cu centers, the mean Mo1···Cu contacts (2.629(3) vs 2.690(3) Å) are similar to those of the corresponding ones in **2** and **3**.



Figure 2. Extended structure of **2** along the [101] direction.



Figure 3. View of a section of the 1D zigzag chain of **3a** (extending along the [101] direction) with labeling scheme. The solvents and the hydrogen atoms were omitted for clarity. Symmetry codes: (A)  $-x, -y + 1, -z + 1$ ; (B)  $-x, -y + 1, -z$ .

Table 2. Selected Bond Distances (Å) and Angles (deg) for **3a**

Mo(1)···Cu(1)	2.6163(15)	Mo(1)···Cu(2)	2.6756(14)
Mo(1)···Cu(3)	2.6960(15)	Mo(1)–S(1)	2.272(3)
Mo(1)–S(3)	2.285(3)	Mo(1)–S(2)	2.302(3)
Cu(1)–S(1)	2.212(3)	Cu(1)–S(2)	2.215(3)
Cu(1)–Br(2)	2.2742(16)	Cu(2)–S(3)	2.234(3)
Cu(2)–N(1)	2.000(7)	Cu(2)–N(3)	2.114(7)
Cu(2)–S(2)	2.237(3)	Cu(3)–S(3)	2.230(3)
Cu(3)–S(1)	2.231(3)	Cu(3)–Br(1)	2.4572(18)
Cu(3)–N(2A)	2.051(8)		
S(1)–Mo(1)–S(3)	104.88(9)	S(1)–Mo(1)–S(2)	105.09(10)
S(3)–Mo(1)–S(2)	105.58(9)	S(1)–Cu(1)–S(2)	110.20(10)
S(1)–Cu(1)–Br(2)	121.26(9)	S(2)–Cu(1)–Br(2)	128.47(9)
N(1)–Cu(2)–N(3)	98.4(3)	N(1)–Cu(2)–S(3)	123.0(2)
N(3)–Cu(2)–S(3)	104.2(2)	N(1)–Cu(2)–S(2)	112.8(2)
N(3)–Cu(2)–S(2)	106.5(2)	S(3)–Cu(2)–S(2)	109.60(10)
N(2A)–Cu(3)–S(3)	109.2(2)	N(2A)–Cu(3)–S(1)	117.2(3)
S(3)–Cu(3)–S(1)	108.17(10)	N(2A)–Cu(3)–Br(1)	98.2(2)
S(3)–Cu(3)–Br(1)	116.91(9)	S(1)–Cu(3)–Br(1)	107.31(8)

The average Mo– $\mu_3$ -S, Cu– $\mu_3$ -S, Cu–N, and terminal Cu–Br distances are normal.

From a topological view, the  $[(\eta^5\text{-C}_5\text{Me}_5)\text{MoS}_3\text{Cu}_3(\mu\text{-bpe})_{0.5}(\text{bpe})\text{Br}_2]$  fragment serves as an angular two-connecting node (node (a)) while the  $[(\eta^5\text{-C}_5\text{Me}_5)\text{MoS}_3\text{Cu}_3(\mu\text{-bpe})_{1.5}\text{Br}_2]$  fragment works as a pyramidal three-connecting node (node (b) in Scheme 1). Two angular two-connecting nodes and four pyramidal three-connecting nodes interconnect through four single bpe bridges and two double bpe bridges, forming a chairlike cyclohexane-shaped unit  $[(\eta^5\text{-C}_5\text{Me}_5)\text{MoS}_3\text{Cu}_3]_6(\mu\text{-bpe})_6(\text{bpe})_2\text{Br}_{12}]$  (Figure 5). The occurrence of an angular two-connecting node and a pyramidal three-connecting node in the same structure is quite rare in cluster-based supramolecular chemistry. The neighbouring cyclohexane-like units are further fused to a unique double-stranded one-dimensional chain extending along the [011] direction (Figure 5). The chains are stacked along the *a* axis to give 1D channels with a cyclohexane-shaped cross section. The effective channel void of 445.0 Å<sup>3</sup> comprises 10.9% of the total cell volume. Although the solvent contribution is

removed because of the severe disorder,<sup>27</sup> they were originally crystallized within the channels (see the Supporting Information).

**Crystal Structure of  $\{[(\eta^5\text{-C}_5\text{Me}_5)\text{MoS}_3\text{Cu}_3]_2(\mu\text{-bpe})_2(\mu\text{-Br})(\mu_3\text{-Br})\text{Br}_2\} \cdot \text{DMF} \cdot \text{MeCN}\}_n$  (**5**).** Compound **5** crystallizes in the triclinic space group  $P\bar{1}$ , and the asymmetric unit contains one independent  $\{[(\eta^5\text{-C}_5\text{Me}_5)\text{MoS}_3\text{Cu}_3]_2(\mu\text{-bpe})_2(\mu\text{-Br})(\mu_3\text{-Br})\text{Br}_2\}$  molecule, one DMF solvent molecule, and one MeCN solvent molecule. As shown in Figure 6, this cluster molecule adopts another kind of double incomplete cubane-like structure in which one  $[(\eta^5\text{-C}_5\text{Me}_5)\text{MoS}_3\text{Cu}_3(\mu\text{-bpe})_{0.5}(\mu\text{-Br})\text{Br}]$  fragment and one  $[(\eta^5\text{-C}_5\text{Me}_5)\text{MoS}_3\text{Cu}_3(\mu\text{-bpe})_{0.5}(\mu_3\text{-Br})\text{Br}]$  fragment are linked by a single bpe bridge. The  $[(\eta^5\text{-C}_5\text{Me}_5)\text{MoS}_3\text{Cu}_3(\mu\text{-bpe})_{0.5}\text{Br}_2]$  fragment assumes a similar incomplete  $\text{MoS}_3\text{Cu}_3$  cubane-like structure to those of **1–4**. The main structural feature for the  $[(\eta^5\text{-C}_5\text{Me}_5)\text{MoS}_3\text{Cu}_3(\mu\text{-bpe})_{0.5}(\mu\text{-Br})\text{Br}]$  fragment consists of a “half-open”  $\text{MoS}_3\text{Cu}_3(\mu\text{-Br})$  cube where the Cu5–Br4 bond is broken, which resembles those of  $[(\eta^5\text{-C}_5\text{Me}_5)\text{WS}_3\text{Cu}_3(\mu\text{-Br})\text{Br}(\text{PPh}_3)_2]^{18d}$  and  $[\text{NET}_4][\text{WOS}_3\text{Cu}_3\text{Br}_4] \cdot 2\text{H}_2\text{O}$ .<sup>28a</sup> The  $[(\eta^5\text{-C}_5\text{Me}_5)\text{MoS}_3\text{Cu}_3(\mu\text{-bpe})_{0.5}(\mu_3\text{-Br})\text{Br}]$  fragment may be viewed as having a severely distorted cubane-like structure, in which one Br atom fills into the void of the incomplete cube of **1a** with one long Cu3–Br2 and two short Cu1–Br2 and Cu2–Br2 distances (Table 4). The resulting  $[(\eta^5\text{-C}_5\text{Me}_5)\text{MoS}_3\text{Cu}_3(\mu_3\text{-Br})]$  cube is closely related to those of  $[(\eta^5\text{-C}_5\text{Me}_5)\text{MoS}_3\text{Cu}_3(\mu_3\text{-Br})(\text{PPh}_3)_3](\text{PF}_6)^{28b}$  and  $[\text{MoOS}_3\text{Cu}_3(\mu_3\text{-Br})(\text{PPh}_3)_3]^{12b}$ . For the  $[(\eta^5\text{-C}_5\text{Me}_5)\text{MoS}_3\text{Cu}_3(\mu\text{-bpe})_{0.5}(\mu_3\text{-Br})\text{Br}]$  fragment, the three Cu atoms are not equivalent, and their coordination variability ranges from a strongly distorted tetrahedron (Cu1 and Cu2) to a nearly trigonal planar coordination (Cu3) with a long Cu3–Br2 interaction (Table 4). Because of the

(27) Spek, A. L. *J. Appl. Crystallogr.* **2003**, *36*, 7–13.

(28) (a) Chen, Z. R.; Hou, H. W.; Xin, X. Q.; Yu, K. B.; Shi, S. *J. Phys. Chem.* **1995**, *99*, 8717–8721. (b) Yu, H.; Zhang, W. H.; Ren, Z. G.; Chen, J. X.; Wang, C. L.; Lang, J. P.; Elim, H. I.; Ji, W. *J. Organomet. Chem.* **2005**, *690*, 4027–4035.

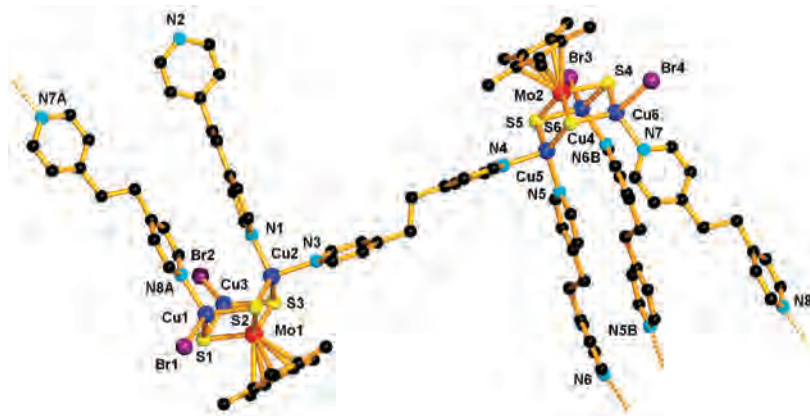


**Figure 4.** View of the  $\{[(\eta^5\text{-C}_5\text{Me}_5)\text{MoS}_3\text{Cu}_3]_2(\mu\text{-bpe})_3(\text{bpe})\text{Br}_4\}$  dimeric structure of **4** with labeling scheme. All hydrogen atoms were omitted for clarity. Symmetry codes: (A)  $x, y - 1, z - 1$ ; (B)  $-x + 1, -y + 3, -z + 2$ .

**Table 3.** Selected Bond Distances (Å) and Angles (deg) for **4**

Mo(1)···Cu(1)	2.700(3)	Mo(1)···Cu(2)	2.676(3)
Mo(1)···Cu(3)	2.629(3)	Mo(2)···Cu(4)	2.696(3)
Mo(2)···Cu(5)	2.672(3)	Mo(2)···Cu(6)	2.705(3)
Mo(1)–S(2)	2.271(6)	Mo(1)–S(3)	2.295(6)
Mo(1)–S(1)	2.297(6)	Mo(2)–S(4)	2.267(6)
Mo(2)–S(5)	2.280(6)	Mo(2)–S(6)	2.294(6)
Cu(1)–S(1)	2.244(6)	Cu(1)–S(2)	2.253(6)
Cu(1)–Br(1)	2.470(4)	Cu(2)–S(2)	2.214(6)
Cu(2)–N(1)	2.050(11)	Cu(2)–N(3)	2.114(9)
Cu(2)–S(3)	2.027(7)	Cu(3)–S(3)	2.210(6)
Cu(3)–S(1)	2.210(6)	Cu(3)–Br(2)	2.281(3)
Cu(4)–S(4)	2.229(7)	Cu(4)–S(5)	2.262(6)
Cu(4)–Br(3)	2.485(4)	Cu(5)–S(5)	2.228(6)
Cu(4)–N(6B)	2.027(7)	Cu(5)–N(5)	2.014(13)
Cu(5)–N(4)	2.105(9)	Cu(6)–N(7)	2.040(12)
Cu(5)–S(6)	2.233(6)	Cu(6)–S(4)	2.235(6)
Cu(6)–S(6)	2.247(6)	Cu(6)–Br(4)	2.520(4)
S(2)–Mo(1)–S(3)	105.0(2)	S(2)–Mo(1)–S(1)	105.6(2)
S(3)–Mo(1)–S(1)	105.3(2)	S(4)–Mo(2)–S(5)	105.6(2)
S(4)–Mo(2)–S(6)	105.2(2)	S(5)–Mo(2)–S(6)	105.5(2)
S(1)–Cu(1)–S(2)	108.0(2)	S(1)–Cu(1)–Br(1)	108.1(2)
N(8A)–Cu(1)–S(1)	115(8)	N(8A)–Cu(1)–S(2)	113(5)
N(8A)–Cu(1)–Br(1)	105(6)	S(2)–Cu(1)–Br(1)	107.34(19)
N(1)–Cu(2)–N(3)	97.0(5)	S(2)–Cu(2)–S(3)	109.1(2)
N(1)–Cu(2)–S(2)	115.9(4)	N(3)–Cu(2)–S(2)	114.0(4)
N(1)–Cu(2)–S(3)	116.2(4)	N(3)–Cu(2)–S(3)	103.5(4)
S(3)–Cu(3)–S(1)	111.3(2)	S(3)–Cu(3)–Br(2)	120.25(19)
S(1)–Cu(3)–Br(2)	128.32(19)	S(4)–Cu(4)–S(5)	107.5(2)
S(4)–Cu(4)–Br(3)	113.3(2)	S(5)–Cu(4)–Br(3)	106.34(19)
N(5)–Cu(5)–S(5)	111.4(5)	S(5)–Cu(5)–S(6)	109.4(2)
N(5)–Cu(5)–N(4)	93.2(6)	N(4)–Cu(5)–S(5)	102.9(4)
N(5)–Cu(5)–S(6)	124.2(5)	N(4)–Cu(5)–S(6)	112.9(4)
S(4)–Cu(6)–S(6)	107.8(2)	S(4)–Cu(6)–Br(4)	102.2(2)
S(6)–Cu(6)–Br(4)	116.61(19)	N(7)–Cu(6)–Br(4)	95.0(5)
N(7)–Cu(6)–S(4)	122.3(5)	N(7)–Cu(6)–S(6)	112.4(5)

different coordination geometries of the Cu atoms, the Mo1···Cu3 contact (2.6462(16) Å) is somewhat shorter than the mean value of the Mo1···Cu1 and Mo1···Cu2 contacts (2.6578(16) Å). For the  $[(\eta^5\text{-C}_5\text{Me}_5)\text{MoS}_3\text{Cu}_3(\mu\text{-bpe})_{0.5}(\mu\text{-Br})\text{Br}]$  fragment, the three Cu centers show more variable coordination geometries from a trigonal planar coordination (Cu5) to a nearly trigonal planar coordination (Cu4) with a long Cu4–Br4 interaction to a distorted tetrahedral coordination (Cu6). It is noted that the Mo2···Cu4 contact is shorter than the other two Mo2···Cu6 contacts and those of **1–4**. The reason may be that the Mo2S4Cu4S5 ring is asymmetric and puckered slightly with a dihedral angle of 17.9° around the Mo2···Cu4 vector, which may lead to the presence of the shorter Mo2···Cu4 contact (2.6184(17) Å). The mean

Cu– $\mu_3$ –Br distance (2.8642(16) Å) in the  $[(\eta^5\text{-C}_5\text{Me}_5)\text{MoS}_3\text{Cu}_3(\mu\text{-bpe})_{0.5}(\mu_3\text{-Br})\text{Br}]$  fragment is longer than those found in  $[(\eta^5\text{-C}_5\text{Me}_5)\text{MoS}_3\text{Cu}_3(\mu_3\text{-Br})(\text{PPh}_3)_3](\text{PF}_6)$  (2.741(1) Å) and  $[\text{MoOS}_3\text{Cu}_3(\mu_3\text{-Br})(\text{PPh}_3)_3]$  (2.653(1) Å). The average Cu– $\mu$ –Br distance (2.7600(18) Å) in the  $[(\eta^5\text{-C}_5\text{Me}_5)\text{MoS}_3\text{Cu}_3(\mu\text{-bpe})_{0.5}(\mu\text{-Br})\text{Br}]$  is longer than that of  $[(\eta^5\text{-C}_5\text{Me}_5)\text{WS}_3\text{Cu}_3(\mu\text{-Br})\text{Br}(\text{PPh}_3)_2]$  (2.647(3) Å). The average Mo– $\mu_3$ –S, Cu– $\mu_3$ –S, Cu–N, and terminal Cu–Br distances are normal. Topologically, each  $[(\eta^5\text{-C}_5\text{Me}_5)\text{MoS}_3\text{Cu}_3]$  core in **5** acts as an angular two-connecting node (node (a)), which bridges its equivalent ones via single bpe bridges to form a single zigzag chain extended along the [110] direction. The 1D chains stacked along the *b* axis to generate 1D channels with rhombic openings of approximately 17.4 × 34.8 Å<sup>2</sup>. The effective solvent accessible volume of 521.2 Å<sup>3</sup> per unit cell (16.5% of the total cell volume) is filled with ordered DMF and MeCN solvents (see the Supporting Information).

**Crystal Structure of  $[(\eta^5\text{-C}_5\text{Me}_5)\text{MoS}_3\text{Cu}_3(\mu\text{-bpp})(\mu\text{-Br})\text{Br}]_n$  (**6**).** Compound **6** crystallizes in the monoclinic space group  $P2_1/c$ , and the asymmetric unit contains a neutral  $[(\eta^5\text{-C}_5\text{Me}_5)\text{MoS}_3\text{Cu}_3(\mu\text{-bpp})(\mu\text{-Br})\text{Br}]$  molecule. As shown in Figure 7, the molecule consists of a “half-open” MoS<sub>3</sub>Cu<sub>3</sub>( $\mu$ -Br) cubane-like structure (where the Cu1–Br1 bond is broken), which is almost the same as that of the  $[(\eta^5\text{-C}_5\text{Me}_5)\text{MoS}_3\text{Cu}_3(\mu\text{-bpe})_{0.5}(\mu\text{-Br})\text{Br}]$  fragment of **5**. The Cu1 atom has trigonal planar coordination geometry while Cu2 and Cu3 show a distorted tetrahedral geometry. The mean Mo(1)···Cu contact, Cu– $\mu$ –Br, Mo– $\mu_3$ –S, Cu– $\mu_3$ –S, Cu–N, and terminal Cu–Br distances are close to those of the corresponding ones of the  $[(\eta^5\text{-C}_5\text{Me}_5)\text{MoS}_3\text{Cu}_3(\mu\text{-bpe})_{0.5}(\mu\text{-Br})\text{Br}]$  fragment of **5** (Table 5).

The  $[(\eta^5\text{-C}_5\text{Me}_5)\text{MoS}_3\text{Cu}_3(\mu\text{-Br})]$  core in **6** works as a two-connecting node (node (a) in Scheme 1) that connects its equivalent ones via the flexible ligand bpp to form a helical chain extended along the *b* axis with a pitch of 26.643 Å (3 times the length of the *b* axis). Three covalently independent and twofold axially related polymeric chains are intertwined into a unique triple-stranded helix through intermolecular C–H···Br hydrogen-bonding interactions (C···Br, 3.77 Å; C–H···Br, 151°) (Figure 8). The separation between the adjacent chains is the same as the length of the *b* axis (8.8707(18) Å). Both the left- and right-handed triple-

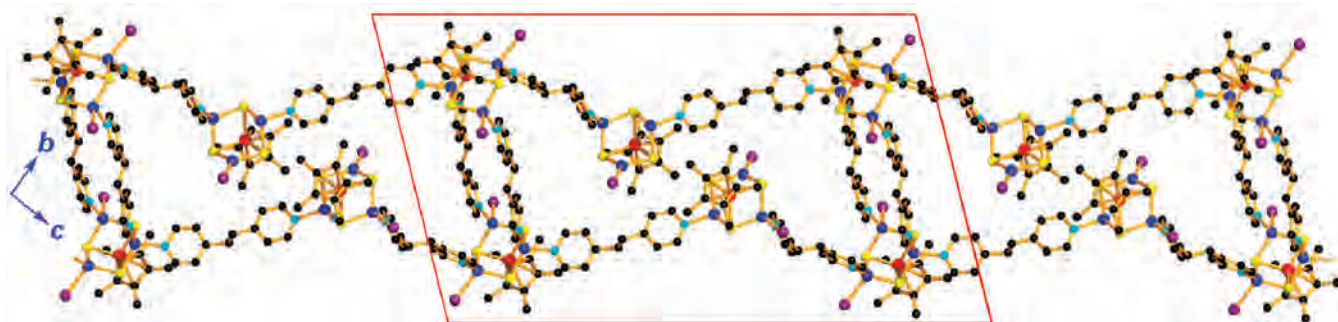


**Figure 5.** View of a section of the double-stranded chain structure of **4** extended along the [011] direction. The chair-conformed hexane-shaped repeating unit was highlighted by the red parallelogram. All hydrogen atoms were omitted for clarity.

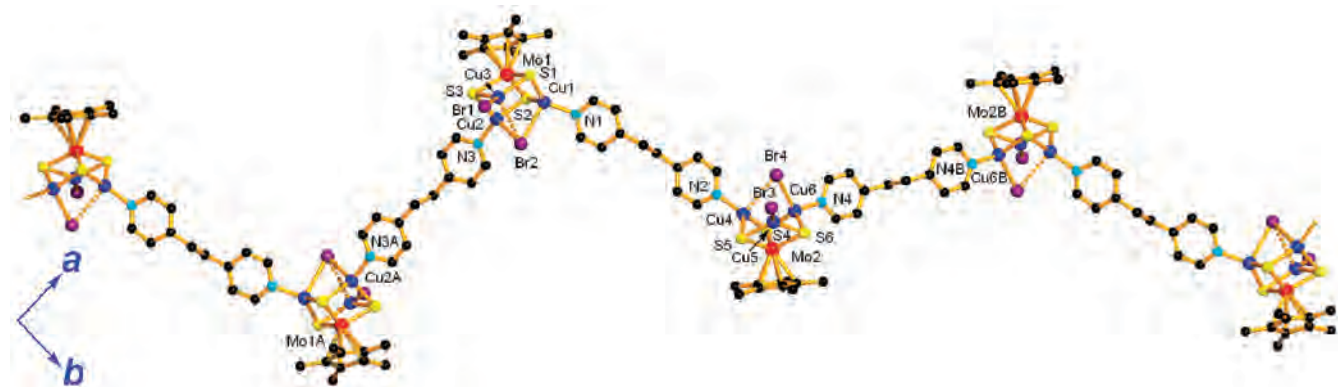


**Figure 6.** View of a section of the 1D zigzag chain (extended along the [110] direction) in **5** with labeling scheme. The solvents and hydrogen atoms were omitted for clarity. Symmetry codes: (A)  $-x + 2, -y + 2, -z + 1$ ; (B)  $-x, -y - 1, -z + 2$ .

stranded helices are racemically packed in the unit cell (see the Supporting Information).

**Table 4.** Selected Bond Distances (Å) and Angles (deg) for **5**

Mo(1)···Cu(1)	2.6552(16)	Mo(1)···Cu(2)	2.6604(16)
Mo(1)···Cu(3)	2.6462(16)	Mo(2)···Cu(4)	2.6184(17)
Mo(2)···Cu(5)	2.6471(16)	Mo(2)···Cu(6)	2.6633(16)
Mo(1)–S(1)	2.282(2)	Mo(1)–S(3)	2.285(2)
Mo(1)–S(2)	2.288(3)	Mo(2)–S(5)	2.278(3)
Mo(2)–S(6)	2.285(3)	Mo(2)–S(4)	2.290(3)
Cu(1)–S(1)	2.228(3)	Cu(1)–S(2)	2.231(3)
Cu(1)–N(1)	1.966(7)	Cu(1)–Br(2)	2.7920(17)
Cu(2)–N(3)	1.982(8)	Cu(2)–S(3)	2.243(3)
Cu(2)–S(2)	2.254(3)	Cu(2)–Br(2)	2.6737(16)
Cu(3)–S(1)	2.227(3)	Cu(3)–S(3)	2.227(3)
Cu(3)–Br(1)	2.3027(19)	Cu(4)–S(4)	2.223(3)
Cu(4)–S(5)	2.230(3)	Cu(4)–N(2)	1.938(8)
Cu(5)–S(6)	2.218(3)	Cu(5)–Br(3)	2.2979(18)
Cu(5)–S(5)	2.217(3)	Cu(6)–N(4)	1.988(8)
Cu(6)–S(4)	2.242(3)	Cu(6)–S(6)	2.256(3)
Cu(6)–Br(4)	2.5432(18)	Cu(4)–Br(4)	2.9768(18)
Cu(3)–Br(2)	3.1259(18)		
S(1)–Mo(1)–S(3)	105.89(10)	S(1)–Mo(1)–S(2)	105.38(10)
S(3)–Mo(1)–S(2)	105.71(9)	S(5)–Mo(2)–S(6)	105.64(10)
S(5)–Mo(2)–S(4)	105.14(10)	S(6)–Mo(2)–S(4)	106.23(10)
S(1)–Cu(1)–S(2)	109.22(10)	S(1)–Cu(1)–Br(2)	104.08(9)
S(2)–Cu(1)–Br(2)	96.05(8)	N(1)–Cu(1)–S(1)	119.7(2)
N(1)–Cu(1)–S(2)	124.0(2)	N(1)–Cu(1)–Br(2)	96.9(2)
S(3)–Cu(2)–S(2)	108.30(10)	S(3)–Cu(2)–Br(2)	107.45(9)
S(2)–Cu(2)–Br(2)	98.86(8)	N(3)–Cu(2)–S(3)	112.1(2)
N(3)–Cu(2)–S(2)	124.7(2)	N(3)–Cu(2)–Br(2)	103.2(2)
S(1)–Cu(3)–S(3)	109.82(10)	S(1)–Cu(3)–Br(1)	124.01(10)
S(3)–Cu(3)–Br(1)	120.69(9)	S(4)–Cu(4)–S(5)	109.08(11)
N(2)–Cu(4)–S(4)	122.0(3)	N(2)–Cu(4)–S(5)	119.6(3)
S(5)–Cu(5)–S(6)	110.14(11)	S(5)–Cu(5)–Br(3)	116.92(9)
S(6)–Cu(5)–Br(3)	129.33(9)	S(4)–Cu(6)–S(6)	108.88(10)
S(4)–Cu(6)–Br(4)	107.31(9)	S(6)–Cu(6)–Br(4)	101.70(9)
N(4)–Cu(6)–S(4)	112.4(3)	N(4)–Cu(6)–S(6)	115.3(3)
N(4)–Cu(6)–Br(4)	110.5(3)		

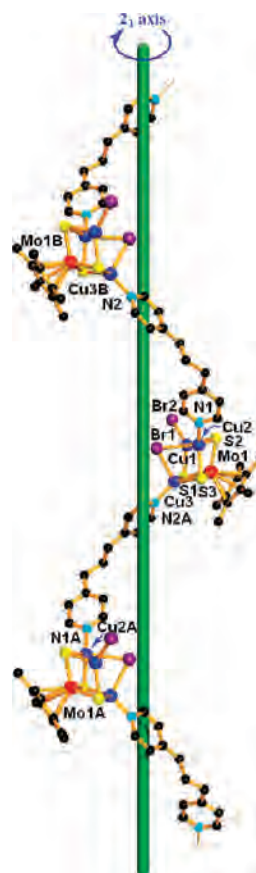


**Figure 7.** View of a section of the 1D helical chain of **6** (extending along the *b* axis) with labeling scheme. Symmetry code: (A)  $-x + 2, y + 3/2, -z + 1/2$ ; (B)  $-x + 2, y - 3/2, -z + 1/2$ .

**Table 5.** Selected Bond Distances (Å) and Angles (deg) for **6**

Mo(1)⋯Cu(1)	2.6496(10)	Mo(1)⋯Cu(2)	2.6524(11)
Mo(1)⋯Cu(3)	2.6501(11)	Mo(1)–S(2)	2.2740(17)
Mo(1)–S(3)	2.2857(19)	Mo(1)–S(1)	2.2948(17)
Cu(1)–S(2)	2.222(2)	Cu(1)–S(1)	2.2348(19)
Cu(1)–Br(2)	2.3038(11)	Cu(2)–S(2)	2.243(2)
Cu(2)–S(3)	2.2569(19)	Cu(2)–Br(1)	2.7999(13)
Cu(2)–N(1)	1.969(5)	Cu(3)–N(2A)	1.977(5)
Cu(3)–S(1)	2.231(2)	Cu(3)–S(3)	2.2429(19)
Cu(3)–Br(1)	2.5973(12)		
S(2)–Mo(1)–S(3)	105.47(6)	S(2)–Mo(1)–S(1)	105.44(6)
S(3)–Mo(1)–S(1)	106.33(7)	S(2)–Cu(1)–S(1)	109.29(7)
S(2)–Cu(1)–Br(2)	116.87(6)	S(1)–Cu(1)–Br(2)	130.44(6)
S(2)–Cu(2)–S(3)	107.49(7)	S(2)–Cu(2)–Br(1)	114.81(6)
N(1)–Cu(2)–S(2)	114.13(17)	N(1)–Cu(2)–S(3)	127.19(17)
N(1)–Cu(2)–Br(1)	99.37(16)	S(3)–Cu(2)–Br(1)	90.97(5)
N(2A)–Cu(3)–S(1)	116.37(17)	N(2A)–Cu(3)–S(3)	119.43(16)
N(2A)–Cu(3)–Br(1)	106.26(16)	S(1)–Cu(3)–S(3)	110.07(7)
S(1)–Cu(3)–Br(1)	104.80(6)	S(3)–Cu(3)–Br(1)	96.75(6)

**Crystal Structure of  $\{[(\eta^5\text{-C}_5\text{Me}_5)\text{MoS}_3\text{Cu}_3]_2(\mu\text{-bpp})_3(\mu\text{-NCS})_2(\text{NCS})\}_n$  (**7**).** Compound **7** crystallizes in the triclinic space group  $P\bar{1}$ , and each asymmetric unit contains the  $\{[(\eta^5\text{-C}_5\text{Me}_5)\text{MoS}_3\text{Cu}_3]_2(\mu\text{-bpp})_3(\mu\text{-NCS})_2(\text{NCS})\}^+$  cluster cation and one  $\text{NCS}^-$  counteranion. The  $\{[(\eta^5\text{-C}_5\text{Me}_5)\text{MoS}_3\text{Cu}_3]_2(\mu\text{-bpp})_3(\mu\text{-NCS})_2(\text{NCS})\}^+$  cluster cation may also be visualized as another kind of double incomplete cubane-like structure, which consists of one  $[(\eta^5\text{-C}_5\text{Me}_5)\text{MoS}_3\text{Cu}_3(\mu\text{-bpp})_{1.5}(\text{NCS})]$  fragment and one  $[(\eta^5\text{-C}_5\text{Me}_5)\text{MoS}_3\text{Cu}_3(\mu\text{-bpp})_{1.5}(\mu\text{-NCS})]$  fragment that are bridged by a single thiocyanate group (Figure 9). Within the two fragments, six unique Cu centers show different coordination environments. Upon being coordinated by two  $\mu_3\text{-S}$  atoms from the  $[(\eta^5\text{-C}_5\text{Me}_5)\text{MoS}_3]$  moiety, Cu1 is coordinated by one terminal NCS to furnish a trigonal planar coordination geometry, while Cu2 and Cu5 are coordinated by two bpp ligands, Cu3 is coordinated by one bpp ligand and one N atom from the bridging thiocyanate group, Cu4 is coordinated by one bpp ligand and one S atom from the bridging thiocyanate group, and Cu6 is coordinated by one N and one S atom from a pair of the bridging thiocyanate groups, forming a distorted tetrahedral coordination geometry. For the trigonally coordinated Cu1 and the tetrahedrally coordinated Cu centers, the mean Mo1⋯Cu1 contacts (2.616(4) vs 2.691(3) Å) are similar to those of the corresponding ones in **2–6**. The average Mo– $\mu_3\text{-S}$ , Cu– $\mu_3\text{-S}$ , and Cu–N distances are normal.

The two cluster fragments serve as two intriguing multiconnecting nodes. The  $[(\eta^5\text{-C}_5\text{Me}_5)\text{MoS}_3\text{Cu}_3(\mu\text{-bpp})_{1.5}(\text{NCS})]$  fragment acts as planar four-connecting node (node (c) in Scheme 1) while the  $[(\eta^5\text{-C}_5\text{Me}_5)\text{MoS}_3\text{Cu}_3(\mu\text{-bpp})_{1.5}(\mu\text{-NCS})]$  fragment works as an unprecedented planar five-connecting node (node (d) in Scheme 1). The two nodes work in a cooperative way to interconnect with the equivalent ones by single and double NCS bridges to give a finite chain extended along the *b* direction. Meanwhile, the resulting finite chain and their symmetry generated motifs are further linked by 12 single bpp bridges to furnish a one-dimensional quadruply stranded chain extending along the *a* axis (Figure 10). The width for this chain is approximately 30.6 Å. Alternatively, two adjacent  $[(\eta^5\text{-C}_5\text{Me}_5)\text{MoS}_3\text{Cu}_3(\mu\text{-bpp})_{1.5}(\mu\text{-NCS})]$  fragments form a centrosymmetric double incomplete cubane-

like motif  $[(\eta^5\text{-C}_5\text{Me}_5)\text{MoS}_3\text{Cu}_3(\mu\text{-bpp})_{1.5}(\mu\text{-NCS})]_2$  through a double thiocyanate bridge. This motif connects its equivalent ones via four single bpp bridges to form a double chain extending along the *a* axis. On the other hand, the  $[(\eta^5\text{-C}_5\text{Me}_5)\text{MoS}_3\text{Cu}_3(\mu\text{-bpp})_{1.5}(\text{NCS})]$  fragment links its neighboring ones via one bpp bridges to form a single chain also extending along the *a* axis. Therefore, two such single chains link the double chain in an opposite direction via single thiocyanate bridges and single bpp bridges to complete this quadruply stranded chain. To our knowledge, such a thick chain has not yet been described. Of the three columns of grids supported by this quadruple structure, the diagonal direction of each grid in two side columns is filled by one additional bpp ligand while the grids in the middle column remain intact. In the unit cell, the chains are arranged in a head-to-tail fashion along the *b* axis to give a zigzag chain, which is further stacked along the *c* direction, 1D channels are thus formed when looking down the *a* axis. A total of 222.2 Å<sup>3</sup> (6.1% of the unit cell volume) void in each unit cell is occupied by the dissociated and disordered  $\text{SCN}^-$  counterions (see the Supporting Information) (Table 6).

**Third-Order Nonlinear Optical (NLO) Properties of **1a**, **2**, **3a**, and **4–7**.** Since the NLO behaviors of **1b** have been described in our earlier report<sup>20g</sup> and **3a** and **3b** are structural analogues, only **1a**, **2**, **3a**, and **4–7** will be used for NLO investigations. The electronic spectra of **1a**, **2**, **3a**, and **4–7** in aniline solution showed relatively low linear absorption in 532 nm (see the Supporting Information), which promises low intensity loss and little temperature change by photon absorption during the NLO measurements. The NLO absorption performances of the aniline solutions of **1a**, **2**, **3a**, and **4–7** were evaluated by the Z-scan technique under an open-aperture configuration at 532 nm (Figure 11). For the pure aniline solvent, the nonlinear transmittance was found to be very large, up to 97.2% (see the Supporting Information), which suggests that its NLO refraction and absorption, if any, have no impact on the NLO properties of the complexes in aniline solution.<sup>20g</sup> Although the detailed mechanism is unknown, it is interesting to note that the NLO absorption data obtained under the conditions used in this work can be well evaluated by literature methods.<sup>29</sup>

The nonlinear absorptive indexes  $\alpha_2$  for these compounds were calculated to be  $7.08 \times 10^{-11} \text{ m}\cdot\text{W}^{-1}$  (**1a**),  $4.80 \times 10^{-11} \text{ m}\cdot\text{W}^{-1}$  (**2**),  $5.43 \times 10^{-11} \text{ m}\cdot\text{W}^{-1}$  (**3a**),  $6.84 \times 10^{-11} \text{ m}\cdot\text{W}^{-1}$  (**4**),  $4.99 \times 10^{-11} \text{ m}\cdot\text{W}^{-1}$  (**5**),  $4.88 \times 10^{-11} \text{ m}\cdot\text{W}^{-1}$  (**6**), and  $4.86 \times 10^{-11} \text{ m}\cdot\text{W}^{-1}$  (**7**), respectively, implying that they have good NLO absorption properties. However, these compounds were not detected to have obvious nonlinear refractive effects, which means that their nonlinear refractive effects were rather weak in our experimental conditions and thus can be neglected.

(29) (a) Sherk-Bahae, M.; Said, A. A.; Wei, T. H.; Hagan, D. J.; Van Stryland, E. W. *IEEE J. Quantum Electron.* **1990**, *26*, 760–769. (b) Sherk-Bahae, M.; Said, A. A.; Van Stryland, E. W. *Opt. Lett.* **1989**, *14*, 955–957.

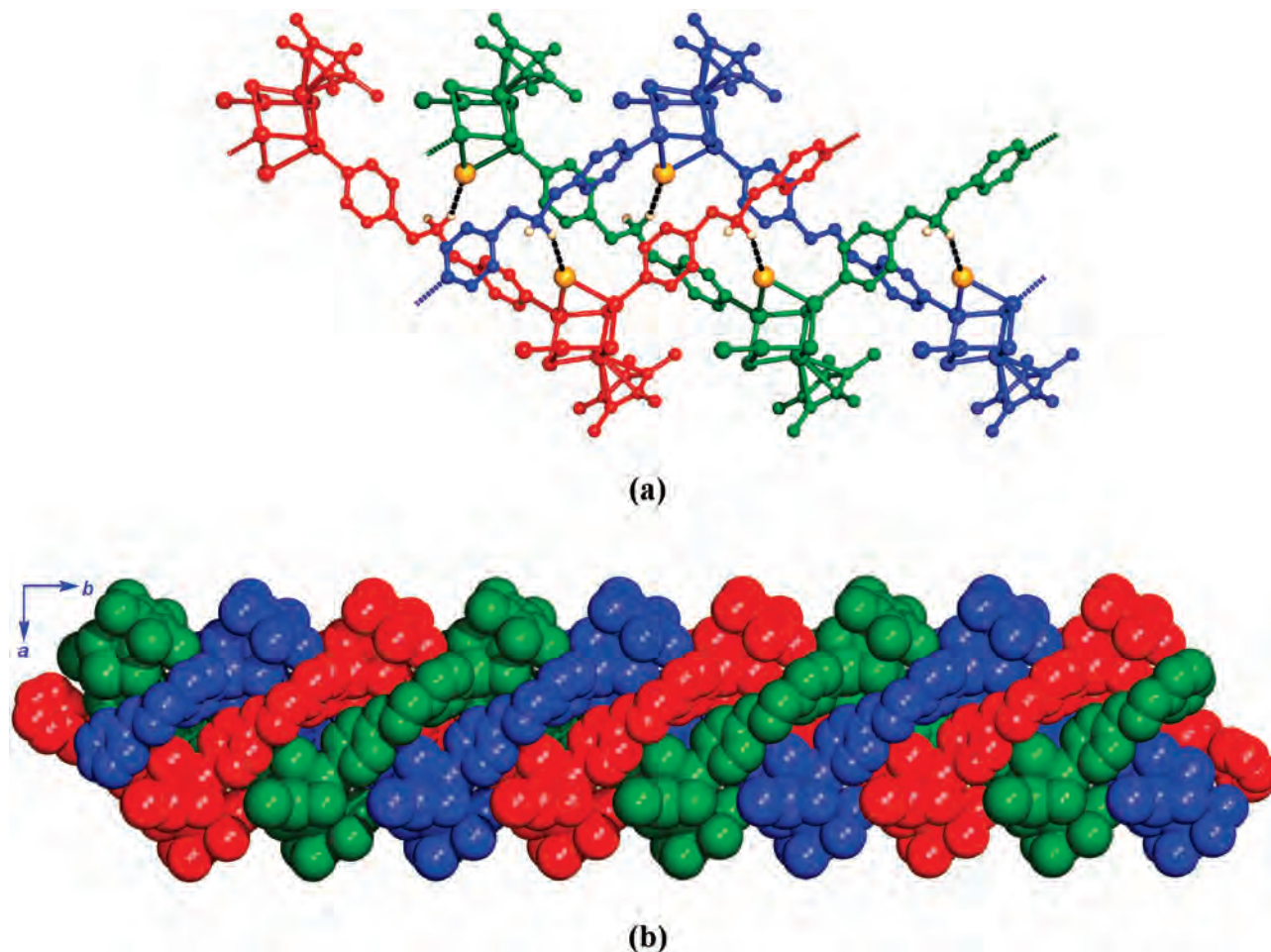


**Figure 8.** (a) View of the C–H···Br hydrogen-bonding interactions (highlighted as black dotted lines) among the three helical chains of **6**. (b) Space filling diagram of the hydrogen-bound triply stranded helix of **6** extending along the *b* axis.

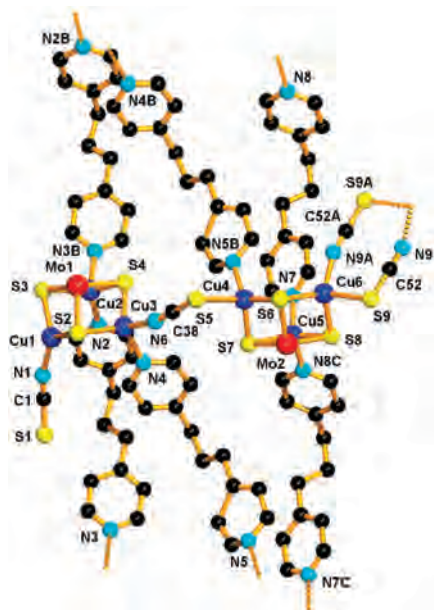


**Figure 9.** Perspective view of the  $[(\eta^5\text{-C}_5\text{Me}_5)\text{MoS}_3\text{Cu}_3]_2(\mu\text{-bpp})_3(\mu\text{-NCS})_2(\text{NCS})^+$  cluster cation in **7** with labeling scheme. The  $\eta^5\text{-C}_5\text{Me}_5$  ligands and the hydrogen atoms were omitted for clarity. Symmetry codes: (A)  $-x + 1, -y + 1, -z + 1$ ; (B)  $x - 1, y, z$ ; (C)  $x + 1, y, z$ .

In accordance with the observed  $\alpha_2$  values, the effective third-order susceptibility<sup>30</sup>  $\chi^{(3)}$  for **1a**, **2**, **3a**, and **4–7** was

calculated to be  $2.86 \times 10^{-12}$  esu (**1a**),  $1.94 \times 10^{-12}$  esu (**2**),  $2.19 \times 10^{-12}$  esu (**3a**),  $2.76 \times 10^{-12}$  esu (**4**),  $2.01 \times 10^{-12}$  esu (**5**),  $1.97 \times 10^{-12}$  esu (**6**), and  $1.96 \times 10^{-12}$  esu (**7**), and the corresponding hyperpolarizabilities  $\gamma$  values<sup>31</sup> were  $5.85 \times 10^{-29}$  esu (**1a**),  $2.98 \times 10^{-29}$  esu (**2**),  $4.00 \times 10^{-29}$  esu (**3a**),  $4.87 \times 10^{-29}$  esu (**4**),  $4.29 \times 10^{-29}$  esu (**5**),  $4.03 \times 10^{-29}$  esu (**6**), and  $3.86 \times 10^{-29}$  esu (**7**), respectively. These results showed that these compounds possess relatively strong third-order optical nonlinearities.

## Conclusion

In this work, we investigated the assembly reactions of **1a** or **1b** with bpe or bpp and isolated a family of  $[(\eta^5\text{-C}_5\text{Me}_5)\text{MoS}_3\text{Cu}_3]$ -supported compounds with one-dimensional arrays (**2–7**). The controlled **1a**-to-bpe ratios were responsible for the formation of five cluster-based complexes with four different kinds of 1D chain structures (**2–5**), which were derived from reactions of the same components (**1a** and bpe). In all these compounds, the cluster core of **1a** or **1b** was retained and acted as multiconnecting nodes under the presence of the bridging bpe, bpp, and

(30) Yang, L.; Dorsinville, R.; Wang, Q. Z.; Ye, P. X.; Alfano, R. R.; Zamboni, R.; Taliani, C. *Opt. Lett.* **1992**, *17*, 323–325.

(31) Chen, Z. R.; Hou, H. W.; Xin, X. Q.; Yu, K. B.; Shi, S. J. *Phys. Chem.* **1995**, *99*, 8717–8721.

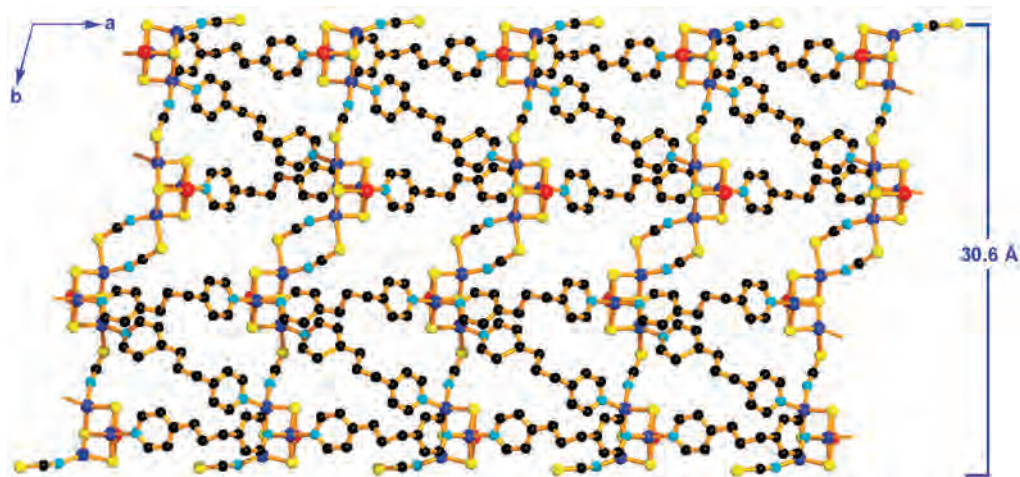


**Figure 10.** View of a section of the 1D chain of **7** (extending along the *a* axis). The  $\eta^5\text{-C}_5\text{Me}_5$  ligands, the  $\text{NCS}^-$  counteranions, and the hydrogen atoms were omitted for clarity.

**Table 6.** Selected Bond Distances (Å) and Angles (deg) for **7**

Mo(1)···Cu(1)	2.616(4)	Mo(1)···Cu(2)	2.691(3)
Mo(1)···Cu(3)	2.682(3)	Mo(2)···Cu(4)	2.681(3)
Mo(2)···Cu(5)	2.704(3)	Mo(2)···Cu(6)	2.696(3)
Mo(1)–S(4)	2.280(6)	Mo(1)–S(3)	2.286(6)
Mo(1)–S(2)	2.292(6)	Mo(2)–S(8)	2.273(5)
Mo(2)–S(6)	2.285(5)	Mo(2)–S(7)	2.276(6)
Cu(1)–N(1)	1.90(2)	Cu(1)–S(2)	2.210(6)
Cu(1)–S(3)	2.221(6)	Cu(2)–N(2)	1.988(15)
Cu(2)–N(3B)	2.084(15)	Cu(2)–S(4)	2.231(6)
Cu(2)–S(3)	2.243(6)	Cu(3)–N(4)	1.986(18)
Cu(3)–N(6)	2.04(2)	Cu(3)–S(2)	2.220(6)
Cu(3)–S(4)	2.233(6)	Cu(4)–N(5B)	2.011(16)
Cu(4)–S(6)	2.224(6)	Cu(4)–S(7)	2.251(6)
Cu(4)–S(5)	2.491(6)	Cu(5)–N(7)	2.04(2)
Cu(5)–N(8C)	2.104(16)	Cu(5)–S(8)	2.238(6)
Cu(5)–S(7)	2.241(6)	Cu(6)–N(9A)	1.949(18)
Cu(6)–S(6)	2.231(5)	Cu(6)–S(8)	2.237(6)
Cu(6)–S(9)	2.589(7)		
S(4)–Mo(1)–S(3)	105.2(2)	S(4)–Mo(1)–S(2)	105.0(2)
S(3)–Mo(1)–S(2)	105.4(2)	S(8)–Mo(2)–S(7)	105.2(2)
S(8)–Mo(2)–S(6)	105.1(2)	S(7)–Mo(2)–S(6)	105.7(2)
N(1)–Cu(1)–S(2)	122.6(6)	N(1)–Cu(1)–S(3)	126.5(6)
S(2)–Cu(1)–S(3)	110.6(2)	N(2)–Cu(2)–N(3B)	103.8(6)
N(2)–Cu(2)–S(4)	117.2(5)	N(3B)–Cu(2)–S(4)	102.1(5)
N(2)–Cu(2)–S(3)	116.1(5)	N(3B)–Cu(2)–S(3)	107.8(5)
S(4)–Cu(2)–S(3)	108.4(2)	N(4)–Cu(3)–N(6)	99.3(8)
N(4)–Cu(3)–S(2)	120.1(6)	N(6)–Cu(3)–S(2)	107.6(5)
N(4)–Cu(3)–S(4)	113.8(6)	N(6)–Cu(3)–S(4)	105.3(5)
S(2)–Cu(3)–S(4)	109.1(2)	N(5B)–Cu(4)–S(6)	125.1(6)
N(5B)–Cu(4)–S(7)	112.9(6)	S(6)–Cu(4)–S(7)	108.7(2)
N(5B)–Cu(4)–S(5)	96.1(6)	S(6)–Cu(4)–S(5)	100.8(2)
S(7)–Cu(4)–S(5)	111.1(2)	N(7)–Cu(5)–N(8C)2	102.6(9)
N(7)–Cu(5)–S(8)	113.9(8)	N(8C)–Cu(5)–S(8)	106.1(5)
N(7)–Cu(5)–S(7)	113.8(8)	N(8C)–Cu(5)–S(7)	112.8(5)
S(8)–Cu(5)–S(7)	107.6(2)	N(9A)–Cu(6)–S(6)	117.3(5)
N(9A)–Cu(6)–S(8)	122.1(6)	S(6)–Cu(6)–S(8)	108.2(2)
N(9A)–Cu(6)–S(9)	97.4(6)	S(6)–Cu(6)–S(9)	110.1(2)
S(8)–Cu(6)–S(9)	98.7(2)		

thiocyanate ligands. In **2**, **3**, **5**, and **6**, each  $[(\eta^5\text{-C}_5\text{Me}_5)\text{MoS}_3\text{Cu}_3]$  core works as an angular two-connecting node to link the equivalent ones through bpe or bpp bridges to form a 1D “Great Wall”-like chain (**2**), a zigzag chain (**3** and **5**), and a helical chain (**6**). Because of the presence of  $\text{C}\cdots\text{H}\cdots\text{Br}$  hydrogen-bonding interactions, **6** shows a 1D H-bonded triply stranded helical chain in its crystal. **4** has a 1D double chain structure in which the  $[(\eta^5\text{-C}_5\text{Me}_5)\text{MoS}_3\text{Cu}_3]$  core serves as a angular two-connecting node and a pyramidal three-connecting node. **7** shows an unprecedented

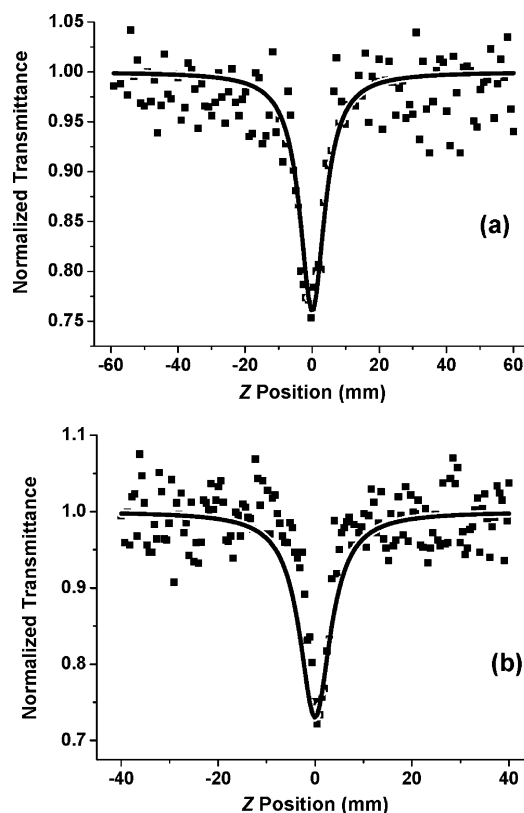


**Figure 11.** Z-scan data for the aniline solutions of  $2.5 \times 10^{-5}$  M for **1a** (a) and  $2.5 \times 10^{-5}$  M for **6** (b). The black solid squares are experimental data, and the solid curves are the theoretical fit.

thick 1D quadruple chain in which the  $[(\eta^5\text{-C}_5\text{Me}_5)\text{MoS}_3\text{Cu}_3]$  core exhibits two unique planar four-connecting and five-connecting nodes. As demonstrated in this paper and previous papers,<sup>20</sup> the ligand effects on the final structure outcomes can be quite complicated. In the case of bpe, the final supramolecular assemblies are not only affected by the ligands but also by the stoichiometric ratios of the reacting components and even the solvents. It is assumed that the low symmetrical ligands like bpe and bpp may induce the  $[(\eta^5\text{-C}_5\text{Me}_5)\text{MoS}_3\text{Cu}_3]$  core to work as irregular connecting nodes, which may result in the formation of less symmetrical

Table 7. Crystallographic Data for 2–7

	2	3a	3b	4	5	6	7
formula	C <sub>64</sub> H <sub>71</sub> Br <sub>4</sub> Cu <sub>6</sub> Mo <sub>2</sub> N <sub>8</sub> S <sub>6</sub>	C <sub>64</sub> H <sub>91</sub> Br <sub>2</sub> Cu <sub>3</sub> MoN <sub>9</sub> OS <sub>7</sub>	C <sub>74</sub> H <sub>89</sub> Br <sub>4</sub> Cu <sub>6</sub> Mo <sub>2</sub> N <sub>11</sub> S <sub>6</sub>	C <sub>68</sub> H <sub>78</sub> Br <sub>4</sub> Cu <sub>6</sub> Mo <sub>2</sub> N <sub>8</sub> S <sub>6</sub>	C <sub>49</sub> H <sub>64</sub> Br <sub>4</sub> Cu <sub>6</sub> Mo <sub>2</sub> N <sub>6</sub> OS <sub>6</sub>	C <sub>23</sub> H <sub>29</sub> Br <sub>2</sub> Cu <sub>3</sub> MoN <sub>3</sub> S <sub>3</sub>	C <sub>126</sub> H <sub>144</sub> Cu <sub>12</sub> Mo <sub>4</sub> N <sub>20</sub> S <sub>20</sub>
fw	2037.41	2109.56	2217.68	2092.50	1838.18	876.04	3726.05
cryst syst	monoclinic	triclinic	triclinic	triclinic	triclinic	monoclinic	triclinic
space group	<i>P</i> 2 <sub>1</sub> / <i>c</i>	<i>P</i> 1	<i>P</i> 1	<i>P</i> 1	<i>P</i> 1	<i>P</i> 2 <sub>1</sub> / <i>c</i>	<i>P</i> 1
<i>a</i> (Å)	18.694(4)	10.857(2)	10.976(2)	11.288(2)	10.027(2)	18.538(4)	12.059(2)
<i>b</i> (Å)	23.853(5)	14.397(3)	14.010(3)	18.141(4)	15.706(3)	8.8707(18)	16.276(3)
<i>c</i> (Å)	16.809(3)	15.052(3)	29.750(6)	20.997(4)	20.198(4)	17.720(4)	19.308(4)
$\alpha$ (deg)	90.98(3)	74.01(3)	97.44(3)	94.63(3)	85.34(3)	106.85(3)	105.64(3)
$\beta$ (deg)		75.42(3)	96.94(3)	100.67(3)	86.70(3)	94.00(3)	94.00(3)
$\gamma$ (deg)		74.51(3)	109.64(3)	103.06(3)	87.41(3)	94.80(3)	94.80(3)
<i>V</i> (Å <sup>3</sup> )	7494(3)	2138.9(9)	4205.7(18)	4082.2(16)	3162.6(11)	2788.9(10)	3619.6(13)
<i>Z</i>	4	2	2	2	2	4	1
<i>D</i> <sub>calcd</sub> (g·cm <sup>-3</sup> )	1.806	1.638	1.751	1.702	1.930	2.086	1.709
$\mu$ (mm <sup>-1</sup> )	4.335	3.824	3.871	5.124	5.124	5.803	2.396
<i>F</i> <sub>000</sub>	4020	1046	2208	2072	1804	1712	1876
reflns collected	47043	20200	40247	26683	30997	26428	25229
unique reflns	7156 ( <i>R</i> <sub>int</sub> = 0.0785)	7755 ( <i>R</i> <sub>int</sub> = 0.0653)	15269 ( <i>R</i> <sub>int</sub> = 0.0478)	7900 ( <i>R</i> <sub>int</sub> = 0.1088)	11490 ( <i>R</i> <sub>int</sub> = 0.0759)	5092 ( <i>R</i> <sub>int</sub> = 0.0651)	7543 ( <i>R</i> <sub>int</sub> = 0.1013)
obsd reflns	6245 ( <i>I</i> > 2 $\sigma$ ( <i>I</i> ))	5822 ( <i>I</i> > 2 $\sigma$ ( <i>I</i> ))	12840 ( <i>I</i> > 2 $\sigma$ ( <i>I</i> ))	5177 ( <i>I</i> > 2 $\sigma$ ( <i>I</i> ))	8740 ( <i>I</i> > 2 $\sigma$ ( <i>I</i> ))	4363 ( <i>I</i> > 2 $\sigma$ ( <i>I</i> ))	5223 ( <i>I</i> > 2 $\sigma$ ( <i>I</i> ))
variables	886	459	903	680	649	312	746
<i>R</i> <sup>a</sup>	0.1091	0.0795	0.0577	0.0992	0.0752	0.0538	0.1027
<i>R</i> <sub>w</sub> <sup>b</sup>	0.2888	0.2051	0.1320	0.2297	0.1026	0.0908	0.2449
GOF <sup>c</sup>	1.155	1.114	1.110	1.101	1.129	1.194	1.237
$\Delta\rho_{\text{max}}$ (e·Å <sup>-3</sup> )	1.252	1.815	1.700	1.271	1.446	0.881	1.981
$\Delta\rho_{\text{min}}$ (e·Å <sup>-3</sup> )	-1.652	-1.035	-1.277	-0.943	-1.015	-0.801	-1.472
<sup>a</sup> <i>R</i> = $\sum  F_o  -  F_c  / \sum  F_o $ . <sup>b</sup> <i>R</i> <sub>w</sub> = $\{w \sum ( F_o  -  F_c )^2 / \sum w  F_o ^2\}^{1/2}$ . <sup>c</sup> GOF = $\{\sum w ( F_o  -  F_c )^2 / (n - p)\}^{1/2}$ , where <i>n</i> is the number of reflections and <i>p</i> is total number of parameters refined.							

cluster-based assemblies. For example, the bpp ligand contains a longer (CH<sub>2</sub>)<sub>*n*</sub> group than bpe and has three more possible conformations (Chart 1). It makes the [( $\eta^5$ -C<sub>5</sub>Me<sub>5</sub>)MoS<sub>3</sub>Cu<sub>3</sub>] core be more complicated connecting nodes (nodes (c) and (d)), thereby forming a more complicated [( $\eta^5$ -C<sub>5</sub>Me<sub>5</sub>)MoS<sub>3</sub>Cu<sub>3</sub>]-supported supramolecular array of 7. Compounds **2**, **3a**, and **4–7** exhibited good third-order NLO properties in solution. However, their NLO performances are similar and not better than those of their precursors **1a** or **1b**, which may be ascribed to the fact that they all have the [( $\eta^5$ -C<sub>5</sub>Me<sub>5</sub>)MoS<sub>3</sub>Cu<sub>3</sub>] core in their structures. It is assumed that the supramolecular arrays derived from the [( $\eta^5$ -C<sub>5</sub>Me<sub>5</sub>)MoS<sub>3</sub>Cu<sub>3</sub>] cores and 4,4'-bipyridine or its derivatives may not greatly enhance the NLO properties. The introduction of more metal ions into such supramolecular arrays may be an efficient way to enhance such properties.<sup>20i</sup> From these results, we concluded that the less symmetric ligands bpe and bpp and **1a** or **1b** may be an excellent combination for the assembly of the [( $\eta^5$ -C<sub>5</sub>Me<sub>5</sub>)MoS<sub>3</sub>Cu<sub>3</sub>]-based polymeric complexes with 1D chain arrays. Further research work on exploring the formation of new 1D cluster-based frameworks by other less symmetric ligands such as 1,4-bis(4-pyridyl)butane (bpb), 1,6-bis(4-pyridyl)hexane (bph) coupled with **1a** or **1b** and the enhancement of their NLO performances is in progress.

## Experimental Section

**General Procedures.** The two cluster precursors [PPh<sub>4</sub>][( $\eta^5$ -C<sub>5</sub>Me<sub>5</sub>)MoS<sub>3</sub>(CuX)<sub>3</sub>] (**1a**: X = Br,<sup>18d</sup> **1b**: X = NCS<sup>20g</sup>) were prepared according to the literature methods, while all other chemicals were used as purchased. Aniline and DMF were freshly distilled under reduced pressure, while other solvents were predried over activated molecular sieves and refluxed over the appropriate drying agents under argon and collected by distillation. The elemental analyses for C, H, and N were performed on a Carlo-Erba CHNO-S microanalyzer. IR spectra were recorded on a Varian 1000 FT-IR spectrometer as KBr disks (4000–400 cm<sup>-1</sup>). UV–vis spectra were measured on a Varian 50 UV–visible spectrophotometer. <sup>1</sup>H NMR spectra were recorded at ambient temperature on a Varian UNITY-400 spectrometer. <sup>1</sup>H NMR chemical shifts were referenced to the deuterated dimethyl sulfoxide (DMSO-*d*<sub>6</sub>) signal.

{[( $\eta^5$ -C<sub>5</sub>Me<sub>5</sub>)MoS<sub>3</sub>Cu<sub>3</sub>]<sub>2</sub>( $\mu$ -bpe)<sub>3.5</sub>Br<sub>4</sub>·MeCN]<sub>*n*</sub> (**2**). A purple-red solution of **1a** (220 mg, 0.2 mmol) in DMF (20 mL) was carefully mixed with a colorless solution of bpe (65 mg, 0.35 mmol) in MeCN (50 mL). The mixture was allowed to stand at room temperature for a few days to afford black prisms of **2**, which were collected by filtration, washed with MeCN and Et<sub>2</sub>O, and dried in air. Yield: 157 mg (70%). Anal. Calcd for C<sub>64</sub>H<sub>75</sub>Br<sub>4</sub>Cu<sub>6</sub>Mo<sub>2</sub>N<sub>8</sub>S<sub>6</sub>: C, 37.65; H, 3.70; N, 5.49. Found: C, 37.43; H, 3.65; N, 5.27. IR (KBr disk): 3034 (w), 2911 (w), 1614 (vs), 1499 (m), 1427 (s), 1377 (s), 1281 (w), 1223 (m), 1150 (m), 1069 (m), 1023 (m), 958 (w), 873 (w), 827 (m), 754 (w), 694 (w), 625 (w), 547 (w), 500 (m), 414 (m) cm<sup>-1</sup>. <sup>1</sup>H NMR (400 MHz, DMSO-*d*<sub>6</sub>):  $\delta$  7.43–8.62 (m, 14H, PyH), 3.05 (s, 7H, CH<sub>2</sub>), 1.97 (s, 15H, C<sub>5</sub>Me<sub>5</sub>).

{[( $\eta^5$ -C<sub>5</sub>Me<sub>5</sub>)MoS<sub>3</sub>Cu<sub>3</sub>]<sub>2</sub>( $\mu$ -bpe)<sub>3</sub>Br<sub>4</sub>·DMSO·3MeCN]<sub>*n*</sub> (**3a**). Compound **3a** was prepared in a manner similar to that described for **2**, by using **1a** (220 mg, 0.2 mmol) in 20 mL of DMSO and bpe (56 mg, 0.3 mmol) in 50 mL of MeCN as starting materials. Black needles of **3a** were collected, washed with MeCN and Et<sub>2</sub>O,

and dried in air. Yield: 161 mg (76%). Anal. Calcd for  $\text{C}_{64}\text{H}_{81}\text{Br}_4\text{Cu}_6\text{Mo}_2\text{N}_9\text{OS}_7$ : C, 36.44; H, 3.87; N, 5.98. Found: C, 36.22; H, 3.80; N, 5.79. IR (KBr disk): 3031 (w), 2907 (w), 1610 (vs), 1560 (w), 1483 (w), 1426 (s), 1378 (m), 1222 (m), 1147 (w), 1056 (m), 1023 (s), 954 (w), 826 (s), 669 (w), 599 (w), 550 (m), 493 (w), 409 (w)  $\text{cm}^{-1}$ .  $^1\text{H NMR}$  (400 MHz,  $\text{DMSO-}d_6$ ):  $\delta$  7.36–8.59 (m, 12H, PyH), 3.01 (m, 6H,  $\text{CH}_2$ ), 1.96 (s, 15H,  $\text{C}_5\text{Me}_5$ ).

$\{[(\eta^5\text{-C}_5\text{Me}_5)\text{MoS}_3\text{Cu}_3]_2(\mu\text{-bpe})_3\text{Br}_4\} \cdot 2\text{aniline} \cdot 3\text{MeCN}$  (**3b**). Compound **3b** was prepared in a manner similar to that described for **2**, by using **1a** (220 mg, 0.2 mmol) in 10 mL of aniline and bpe (56 mg, 0.3 mmol) in 50 mL of MeCN as starting materials. Black plates of **3b** were collected, washed with aniline, MeCN, and  $\text{Et}_2\text{O}$ , and dried in air. Yield: 161 mg (72%). Anal. Calcd for  $\text{C}_{74}\text{H}_{89}\text{Br}_4\text{Cu}_6\text{Mo}_2\text{N}_{11}\text{S}_6$ : C, 40.08; H, 4.05; N, 6.95. Found: C, 39.85; H, 4.00; N, 6.76. IR (KBr disk): 3039 (w), 2936 (w), 2253 (m), 1932 (w), 1603 (vs), 1500 (s), 1468 (w), 1373 (m), 1281 (s), 1175 (m), 1056 (w), 1038 (s), 996 (w), 755 (m), 694 (s), 620 (w), 507 (m), 411 (w)  $\text{cm}^{-1}$ .  $^1\text{H NMR}$  (400 MHz,  $\text{DMSO-}d_6$ ):  $\delta$  7.24–8.45 (m, 12H, PyH), 3.03 (s, 6H,  $\text{CH}_2$ ), 2.01 (s, 15H,  $\text{C}_5\text{Me}_5$ ).

$\{[(\eta^5\text{-C}_5\text{Me}_5)\text{MoS}_3\text{Cu}_3]_2(\mu\text{-bpe})_3(\text{bpe})\text{Br}_4\} \cdot 0.35\text{DMF}$  (**4**). Compound **4** was prepared in a manner similar to that described for **2**, using **1a** (220 mg, 0.2 mmol) and bpe (74 mg, 0.4 mmol) as starting materials. Black square thin plates of **4** were collected, washed with MeCN and  $\text{Et}_2\text{O}$ , and dried in air. Yield: 102 mg (48%). Anal. Calcd for  $\text{C}_{69}\text{H}_{80.5}\text{Br}_4\text{Cu}_6\text{Mo}_2\text{N}_{8.35}\text{O}_{0.35}\text{S}_6$ : C, 39.14; H, 3.83; N, 5.52. Found: C, 39.08; H, 3.77; N, 5.39. IR (KBr disk): 3045 (w), 2909 (w), 1674 (m), 1611 (vs), 1558 (w), 1498 (m), 1426 (s), 1378 (s), 1223 (m), 1070 (m), 1015 (s), 827 (s), 814 (s), 667 (w), 599 (w), 549 (m), 518 (w), 412 (m)  $\text{cm}^{-1}$ .  $^1\text{H NMR}$  (400 MHz,  $\text{DMSO-}d_6$ ):  $\delta$  7.40–8.54 (m, 16H, PyH), 3.06 (s, 8H,  $\text{CH}_2$ ), 1.96 (s, 15H,  $\text{C}_5\text{Me}_5$ ).

$\{[(\eta^5\text{-C}_5\text{Me}_5)\text{MoS}_3\text{Cu}_3]_2(\mu\text{-bpe})_2(\mu\text{-Br})(\mu_3\text{-Br})\text{Br}_2\} \cdot \text{DMF} \cdot \text{MeCN}$  (**5**). Compound **5** was prepared in a manner similar to that described for **2**, by using **1a** (220 mg, 0.2 mmol) and bpe (37 mg, 0.2 mmol) as starting materials. Black plates of **5** were collected, washed with MeCN and  $\text{Et}_2\text{O}$ , and dried in air. Yield: 144 mg (78%). Anal. Calcd for  $\text{C}_{49}\text{H}_{64}\text{Br}_4\text{Cu}_6\text{Mo}_2\text{N}_6\text{OS}_6$ : C, 32.02; H, 3.51; N, 4.57. Found: C, 31.90; H, 3.48; N, 4.25. IR (KBr disk): 3031 (w), 2907 (w), 1664 (m), 1610 (vs), 1558 (w), 1485 (w), 1427 (s), 1384 (m), 1222 (m), 1147 (w), 1070 (m), 1023 (m), 878 (w), 825 (m), 624 (w), 551 (m), 496 (w), 414 (w)  $\text{cm}^{-1}$ .  $^1\text{H NMR}$  (400 MHz,  $\text{DMSO-}d_6$ ):  $\delta$  7.38–8.45 (m, 12H, PyH), 3.04 (m, 6H,  $\text{CH}_2$ ), 1.95 (s, 15H,  $\text{C}_5\text{Me}_5$ ).

$(\eta^5\text{-C}_5\text{Me}_5)\text{MoS}_3\text{Cu}_3(\mu\text{-bpp})(\mu\text{-Br})\text{Br}$  (**6**). Compound **6** was prepared in a manner similar to that described for **2**, by using **1a** (220 mg, 0.2 mmol) in 20 mL of DMF and bpp (60 mg, 0.3 mmol) in 50 mL of MeCN as starting materials. Black block crystals of **6** were collected, washed with MeCN and  $\text{Et}_2\text{O}$ , and dried in air. Yield: 112 mg (64%). Anal. Calcd for  $\text{C}_{23}\text{H}_{29}\text{Br}_2\text{Cu}_3\text{MoN}_2\text{S}_3$ : C, 31.53; H, 3.34; N, 3.20. Found: C, 31.82; H, 3.28; N, 3.35. IR (KBr disk): 2949 (w), 2915 (w), 2860 (w), 1616 (vs), 1582 (s), 1499 (s), 1428 (s), 1376 (s), 1288 (m), 1220 (m), 1068 (w), 1022 (m), 817 (m), 754 (s), 694 (m), 623 (w), 509 (m), 415 (m)  $\text{cm}^{-1}$ .  $^1\text{H NMR}$  (400 MHz,  $\text{DMSO-}d_6$ ):  $\delta$  6.55–7.26 (m, 8H, PyH), 2.06–2.66 (m, 6H,  $\text{CH}_2$ ), 1.92 (s, 15H,  $\text{C}_5\text{Me}_5$ ).

$\{[(\eta^5\text{-C}_5\text{Me}_5)\text{MoS}_3\text{Cu}_3]_2(\mu\text{-bpp})_3(\mu\text{-NCS})_2(\text{NCS})\}(\text{NCS})$  (**7**). Compound **7** was prepared in a manner similar to that described for **2**, by using **1b** (206 mg, 0.2 mmol) in 20 mL of DMF and bpp (60 mg, 0.3 mmol) in 50 mL of MeCN as starting materials. Black plates of **7** were collected, washed with MeCN and  $\text{Et}_2\text{O}$ , and dried in air. Yield: 145 mg (78%). Anal. Calcd for  $\text{C}_{63}\text{H}_{72}\text{Cu}_6\text{Mo}_2\text{N}_{10}\text{S}_{10}$ : C, 40.61; H, 3.89; N, 7.52. Found: C, 40.42; H, 3.98; N, 7.63. IR

(KBr disk): 2942 (w), 2919 (w), 2101 (vs), 2079 (br,s), 1932 (w), 1614 (vs), 1558 (w), 1425 (s), 1384 (m), 1376 (m), 1223 (w), 1084 (m), 1068 (m), 1020 (w), 814 (m), 795 (w), 669 (w), 614 (w), 515 (m), 408 (w)  $\text{cm}^{-1}$ .  $^1\text{H NMR}$  (400 MHz,  $\text{DMSO-}d_6$ ):  $\delta$  7.70–7.98 (m, 24H, PyH), 2.01–2.59 (m, 18H,  $\text{CH}_2$ ), 1.90 (s, 30H,  $\text{C}_5\text{Me}_5$ ).

**X-ray Structure Determination.** X-ray quality crystals of **2–7** were obtained directly from the above preparations. The measurements of **2–7** were made on a Rigaku Mercury CCD X-ray diffractometer by using graphite-monochromated Mo  $\text{K}\alpha$  ( $\lambda = 0.71073$  Å). Single crystals were mounted with grease at the top of a glass fiber and cooled at 193 K in a liquid  $\text{N}_2$  stream. Cell parameters were refined by using the program CrystalClear (Rigaku and MSC, version 1.3, 2001). The collected data were reduced by using the program CrystalStructure (Rigaku and MSC, version 3.60, 2004) while an absorption correction (multiscan) was applied. The reflection data were also corrected for Lorentz and polarization effects.

The crystal structures of **2–7** were solved by direct methods and refined on  $F^2$  by full-matrix least-squares techniques with the SHELXTL-97 program.<sup>32</sup> For **2**, the two bpe ligands and the two  $\eta^5\text{-C}_5\text{Me}_5$  ligands were found to be disordered over two sites with an occupancy factor of 0.53/0.47 for N5/N5A, C25–C36/C25A–C36A, and N6/N6A, or 0.19/0.81 for N7/N7A and C40–C41/C40A–C41A, or 0.58/0.42 for C43–C52/C43A–C52A, or 0.37/0.63 for C53–C62/C53A–C62A. For **3a**, the site occupation factor for the DMSO solvent molecule and one of the MeCN solvent molecules were fixed to be 0.5 to give reasonable temperature factors. For **4**, the solvent accessible void occupies a volume of 444.2 Å<sup>3</sup> (10.9% of the total cell volume) and is filled with highly disordered DMF solvents based on the FT-IR spectra. Since disorder models did not give satisfactory results, the solvent contribution to the scattering factors has been taken into account with PLATON/SQUEEZE.<sup>27</sup> A total of 28 electrons were found in each unit cell, corresponding to 0.70DMF molecules per cell. Where relevant, the crystal data reported in this paper are without the contribution of the disordered solvent molecules. By taking into account the partial occupation of the DMF solvent molecules, the following values were obtained for those parameters:  $\text{C}_{68}\text{H}_{78}\text{Br}_4\text{Cu}_6\text{Mo}_2\text{N}_8\text{S}_6 \cdot 0.35\text{DMF}$  ( $Z = 2$ ),  $\text{fw} = 2118.09$ ,  $\mu = 3.983$   $\text{mm}^{-1}$ ,  $F_{000} = 2100.0$ , and  $D_{\text{calcd}} = 1.723$   $\text{g/cm}^3$ . For **7**, one of the bpp ligands was split into two positions with an occupancy factor of 0.5/0.5 for C20–C23/C20A–C23A and C26–C27/C26A–C27A. The  $\text{NCS}^-$  counteranions were disordered over two orientations with an occupancy factor of 0.5/0.5. All non-hydrogen atoms, except for those of one disordered bpe ligand (N7, C37–C42, N7A, and C40A–C42A) and the MeCN solvent molecules in **2**, and those of the disordered  $\text{NCS}^-$  counteranions in **7**, were refined anisotropically. For **2**, the hydrogen atoms for one disordered bpe (C37, C38, C40, C41, C40A, and C41A) were not located. For **3b**, the hydrogen atoms for  $\text{NH}_2$  groups of the solvent aniline were located from a Fourier map, and their N–H distances were restrained to be equal. Other hydrogen atoms were placed in geometrically idealized positions (C–H = 0.98 Å with  $U_{\text{iso}}(\text{H}) = 1.5U_{\text{eq}}(\text{C})$  for methyl groups; C–H = 0.99 Å with  $U_{\text{iso}}(\text{H}) = 1.2U_{\text{eq}}(\text{C})$  for methylene groups; C–H = 0.95 Å with  $U_{\text{iso}}(\text{H}) = 1.2U_{\text{eq}}(\text{C})$  for aromatic rings) and constrained to ride on their parent atoms. A summary of the key crystallographic information for **2–7** are listed in Table 7.

**Third-Order Nonlinear Optical (NLO) Measurements of 1a, 2, 3a, and 4–7.** The aniline solutions of **1a** ( $2.5 \times 10^{-5}$  M), **2** ( $3.3 \times 10^{-5}$  M), **3a** ( $2.8 \times 10^{-5}$  M), **4** ( $2.9 \times 10^{-5}$  M), **5** ( $2.4 \times 10^{-5}$  M), **6** ( $2.5 \times 10^{-5}$  M), and **7** ( $2.6 \times 10^{-5}$  M) were placed in

(32) Sheldrick, G. M. *SHELXS-97 and SHELXL-97, Program for X-ray Crystal Structure Solution*; University of Göttingen: Göttingen, Germany, 1997.

a 2 mm quartz cuvette for the third-order NLO measurements. These compounds were stable toward air and laser light under experimental conditions. The nonlinear absorption was investigated with a linear polarized laser light ( $\lambda = 532$  nm; pulse widths = 4.5 ns; repetition rate = 2 Hz) generated from a frequency-doubled, mode-locked, Q-switched Nd:YAG laser. The spatial profiles of the optical pulses were nearly Gaussian after passing through a spatial filter. The laser beam was focused with a 30 cm focal length focusing mirror. The radius of the beam waist was measured to be 32  $\mu\text{m}$  (half-width at  $1/e^2$  maximum). The incident and transmitted pulse energies were measured simultaneously by two energy detectors (Laser Precision Rjp-735), which were linked to a computer by an IEEE interface. The NLO properties of the samples were manifested by moving the samples along the axis of the incident laser irradiance beam (Z-direction) with respect to the focal point and with incident laser irradiance kept constant (Z-scan methods).<sup>29</sup> The closed-aperture curves of 0.2 mm radius were placed in front of the detector to measure the transmitted energy when an assessment of laser beam

distortion was needed. To eliminate scattering effects, a lens was mounted after the samples to collect the scattered light.

**Acknowledgment.** This work was supported by the National Natural Science Foundation of China (20525101), the Specialized Research Fund for the Doctoral Program of Higher Education (20050285004), the State Key Laboratory of Organometallic Chemistry of Shanghai Institute of Organic Chemistry (06-26), the Qin-Lan Project of Jiangsu Province, and Program for Innovative Research Team of Soochow University. We are grateful to the reviewers for their helpful suggestions.

**Supporting Information Available:** Crystallographic data of compounds 2–7 (CIF format), cell packing diagrams for 2–7, UV–vis spectra for 1a, 2, 3a, and 4–7, Z-scan data for 2, 3a, 4, 5, 7 and pure aniline in PDF format. This material is available free of charge via the Internet at <http://pubs.acs.org>.

IC8003454